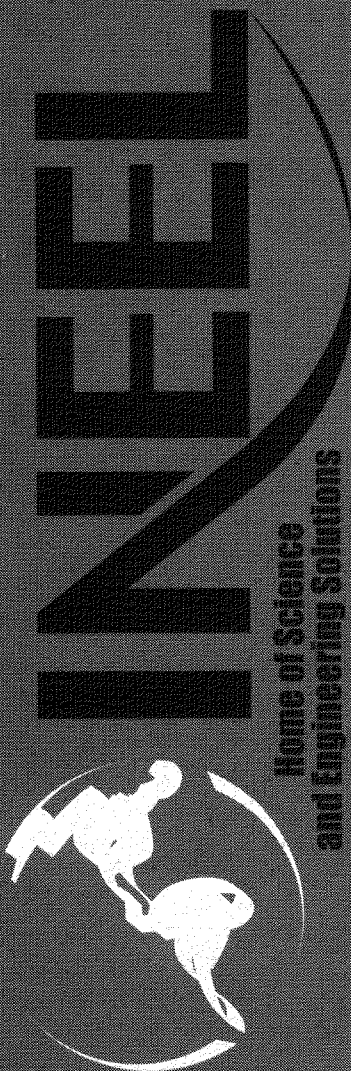


Fate of Magnesium Chloride Brine Applied to Suppress Dust from Unpaved Roads at the INEEL Subsurface Disposal Area

*Larry C. Hull
Carolyn W. Bishop
June 2003*



*Idaho National Engineering and Environmental Laboratory
Bechtel/BWXT Idaho, LLC*

Fate of Magnesium Chloride Brine Applied to Suppress Dust from Unpaved Roads at the INEEL Subsurface Disposal Area

Larry C. Hull
Carolyn W. Bishop

June 2003

**Idaho National Engineering and Environmental Laboratory
Biological and Geological Sciences Department
Idaho Falls, Idaho 83415**

**Prepared for the
U.S. Department of Energy
Assistant Secretary for Environmental Management
Under DOE Idaho Operations Office
Contract DE-AC07-99ID13727**

ABSTRACT

The objective of this investigation is to evaluate the distribution and persistence of chloride in the vadose zone within the radioactive waste Subsurface Disposal Area at the Idaho National Engineering and Environmental Laboratory following the application of magnesium chloride brine on unpaved roads for dust suppression. The interest arises because chloride ions can accelerate the corrosion of metals, which could lead to a more rapid release of radionuclides from metal waste containers and activated metals buried at the site. While most roads where brine was applied were not over buried waste, maps of brine application show that brine was applied to roads that cross directly over buried waste in four locations.

An estimated 660 tons of brine were applied in four applications between 1984 and 1993, contributing 178 tons of chloride to the Subsurface Disposal Area. An electromagnetic induction survey of ground conductivity showed that roadbeds and drainage ditches beside roads had higher ground conductivity than background 7 years after brine was applied to roads. Sediment samples were collected from auger holes drilled through roadbeds and drainage ditches and analyzed for soluble ions 3 years after the last brine application. Elevated chloride concentrations were found to depths of 6.5 ft in roadbed material. In drainage ditches where recharge of surface water is high, chloride has been flushed from the sediments. In areas of lower recharge, chloride remains in the sediments under the drainage ditches. Water samples collected from suction lysimeters were analyzed for dissolved ions to evaluate the spatial and temporal distribution of brine. Solutes from the brine were found in suction lysimeters adjacent to roadways where brine was applied.

From the lateral spread of brine to lysimeters and auger holes, brine has spread laterally up to 40 ft in unsaturated sediments along roadways. Most shallow lysimeters, depth < 23 ft, and one lysimeter at 43 ft depth, show declines in chloride concentration indicating the brine is being leached from the near-surface sediments. Vertical brine movement is directly related to the amount of surface water recharge through sediments. The brine migrated rapidly downward, and has penetrated the subsurface to depths of 220 ft in a few locations. Vertical migration rates can only be bounded because first arrival was not measured. Chloride from brine was measured at a depth of 89 ft after 5.7 years and 220 ft after 5.4 years. The distribution of chloride in sediments and pore water is consistent with estimates of the spatial distribution of surface water recharge and vadose zone residence times from other investigations.

CONTENTS

ABSTRACT	iii
ACRONYMS	xi
1. INTRODUCTION	1
2. SITE DESCRIPTION	2
2.1 Meteorology and Climatology	3
2.2 Geology	3
2.3 Hydrology	5
2.3.1 Surface Water Hydrology	5
2.3.2 Vadose Zone Hydrology	6
2.3.3 Perched Water.....	7
3. MAGNESIUM CHLORIDE BRINE TREATMENTS	8
3.1 Brine Chemistry	8
3.2 Brine Application	8
4. BRINE IN VADOSE ZONE PORE WATER	12
4.1 Vadose Zone Monitoring Network	12
4.2 Vadose Zone Pore-Water Chemistry	14
4.2.1 Shallow Vadose Zone	14
4.2.2 Intermediate Vadose Zone	29
4.2.3 Deep Vadose Zone	32
5. MIGRATION RATES.....	34
6. GASES	35
6.1 Oxygen	35
6.2 Carbon Dioxide	36
7. PERSISTENCE OF BRINE IN SEDIMENTS	37
7.1 Ground Conductivity Survey	37
7.2 SDA Surficial Sediment Samples	39
7.2.1 Site Selection	39
7.2.2 Laboratory Methods	41

7.3	Extractable Cation and Anion Data.....	41
7.3.1	Soluble Chloride Distribution in Sediments	42
7.3.2	Comparison of Soluble and Dissolved Chloride Concentrations.....	45
8.	DISCUSSION	48
9.	REFERENCES	50
Appendix A—Suction Lysimeters Installed at the Radioactive Waste Management Complex		A-1
Appendix B—Physical and Chemical Characteristics of Representative Water Samples from the Shallow and Intermediate Depths in the Vadose Zone at the SDA		B-1
Appendix C—Concentrations of Extractable Soluble Salts in Surficial Sediment Samples Collected from the SDA		C-1

FIGURES

1.	Map of showing the location of the INEEL in southeastern Idaho and the location of the Radioactive Waste Management Complex	2
2.	Cross-section trending west to east through the Subsurface Disposal Area	4
3.	Map of the Subsurface Disposal Area showing the distribution of ponded water from snow-melt in the Spring of 1995	6
4.	Map showing the SDA roads that were treated with dust suppressant in 1984, 1985, and 1992. No map is available for the 1993 brine treatment. The map also shows the locations of pits and trenches in the SDA, and shows that brine was applied directly over some of the waste disposal locations.....	10
5.	Locations of wells where suction lysimeters are installed at the Subsurface Disposal Area	13
6.	Piper diagram of waters in the shallow vadose zone. The star represents the magnesium chloride brine applied to roads, the squares are samples contaminated by brine, and the circles are the unaffected waters. Symbol size in the triangle is proportional to chloride concentration, except for the brine symbol	16
7.	Correlation of chloride concentration to bromide concentration for water samples from the surficial sediment and for the brine applied to the roads	17
8.	Correlation of chloride concentration to bromide concentration for water samples from the surficial sediment.....	17
9.	Correlation of chloride concentration to magnesium concentration for water samples from the surficial sediment and the brine applied to roads	18
10	Correlation of chloride concentration to magnesium concentration for water samples from the surficial sediment.....	18

11.	Correlation of chloride concentration to sodium concentration for water samples from the surficial sediment and the brine applied to roads	19
12.	Correlation of chloride concentration to sulfate concentration for water samples from surficial sediment and the brine applied to the roads	19
13.	Correlation of chloride concentration to sulfate concentration for water samples from the surficial sediment.....	20
14.	Piper plot of water chemistry in the shallow vadose zone showing the evolution of water contaminated by brine as it picks up sulfate and sodium relative to the dilution of the water by in-situ pore water	22
15.	Map of the SDA showing the distribution of wells in the shallow vadose zone contaminated by magnesium chloride brine	23
16.	Time series plot of chloride concentrations in the south east corner of the SDA in wells 98-1, W05. and LYS-1	24
17.	Time series plot of sulfate concentrations in the south-east corner of the SDA in wells 98-1 and W05	25
18.	Time series pot of chloride concentrations in lysimeters at the southeast corner of the SDA that do not show brine contamination	25
19.	Time series plot of chloride concentrations at the west end of the SDA in wells W23 and 98-5	26
20.	Time series plot of sulfate concentrations in the west end of the SDA in wells W23 and 98-5	26
21.	Time series plot of chloride concentrations near Pad A	27
22.	Time series plot of sulfate concentrations near Pad A	27
23.	Time series plot of nitrate-N concentrations near Pad A for all reported nitrate data. Most of the fluctuations between sampling episodes vary by a factor of about 4.4 suggesting that the variation is from reporting units rather than changes in water chemistry	28
24.	Time series plot of selected nitrate-N concentrations near Pad A	28
25.	Piper diagram of waters in the intermediate vadose zone. The star represents the magnesium chloride brine. the squares are samples contaminated by the brine. and the circles are the unaffected waters. Symbol size in the triangle is proportional to chloride concentration. except for the brine	29
26.	Map of the SDA showing the distribution of wells in the intermediate vadose zone contaminated by magnesium chloride brine	31
27.	Time series plot of chloride concentrations in the intermediate vadose zone near Pad A.....	31
28.	Time series plot of sulfate concentrations in the intermediate vadose zone near Pad A	32

29.	Map of the SDA showing the distribution of wells in the deep vadose zone contaminated by magnesium chloride brine	33
30.	Map of the SDA showing the locations of the wells where dissolved oxygen has been measured and the concentrations of dissolved oxygen in mg/L. Water in equilibrium with air at an elevation of 5,000 ft would contain about 8.5 mg/L.....	35
31.	Map of the SDA showing the calculated partial pressure of carbon dioxide in ppmv in lysimeter water. The partial pressure of carbon dioxide in air is about 360 ppmv	36
32.	Map of sediment conductivity of the SDA measured in 1992 using electromagnetic induction	38
33.	Map of the SDA showing the locations of wells where sediments were collected for analysis of soluble ions	40
34.	Distribution of extractable chloride, in mg/kg, with depth along the main east-west haul road. The scale of the graphs is 0–200 mg/kg	43
35.	Distribution of extractable chloride, in mg/kg, with depth from the central portion of the SDA around Pits 4, 10, 13 and the Acid Pit. The scale of the graphs is 0–200 mg/kg. To show more detail at low concentrations, some of the higher concentrations are truncated. Information for higher concentrations is shown in the attached table	44
36.	Distribution of extractable chloride with depth along the southern boundary of the SDA. The scale of the graphs is 0–2,000 mg/kg, or 10x the scale in the previous figures	45
37.	Correlation between dissolved chloride and soluble chloride in SDA sediments	47

TABLES

1.	Chemical composition of magnesium chloride brine applied to SDA	8
2.	Estimates of the total kilograms of brine applied to roads in and around the SDA.....	11
	Summary statistics for water samples collected from suction lysimeters in the shallow vadose zone at the SDA.....	15
4.	Calculation of ion gains and losses relative to chloride from the original brine. Concentrations in meq/L	21
5.	Precipitation-weighted average chemical composition of atmospheric deposition at Craters of the Moon National Monument for the period 1980 to 2000.	23
6.	Distances from wells to the nearest road	23
7.	Summary statistics for water samples collected from suction lysimeters in the intermediate vadose zone at the SDA.....	30
8.	Summary statistics for water samples collected from suction lysimeters in the deep vadose zone at the SDA.....	32

9.	Estimates of water percolation rates for perched water wells and lysimeters completed in the intermediate and deep vadose zone	34
10.	Average of the absolute value of the RPD for the soluble ion extractions	42
11.	Comparison of soluble chloride extracted from sediments and dissolved chloride collected from suction lysimeters for data collected at comparable depths	46

ACRONYMS

INEEL	Idaho National Engineering And Environmental Laboratory
RPD	relative percent difference
RWMC	Radioactive Waste Management Complex
SDA	Subsurface Disposal Area
SVR	soil vault row
TSA	Transuranic Storage Area

Fate of Magnesium Chloride Brine Applied to Suppress Dust from Unpaved Roads at the INEEL Subsurface Disposal Area

1. INTRODUCTION

The application of brine to unpaved roads as a stabilizing agent provides significant benefits for reduction in maintenance costs, control of particulate air emissions, and reduction of storm-water runoff pollution (Hansen 1982; Skorseth 2000). Salt from road application can also have negative effects by increasing the conductivity of runoff water, which induces and accelerates corrosion (Keating 2001). Corrosion can affect critical vehicle parts, damage bridge decks, and can compromise the structural integrity of parking structures (Transportation Research Board 1991). Chloride ions penetrate concrete and corrode reinforcing rods, causing the surrounding concrete to crack and fragment. Other roadside hardware and some nonhighway objects near salt-treated roads are also affected by the corrosive properties of road salts (Transportation Research Board 1991).

The enhancement of corrosion by salt is also a concern for the disposal of radioactive waste. Waste containers used for the disposal of radioactive waste and buried activated metals are subject to degradation by underground corrosion (Piciulo, Shea, and Barletta 1985). Corrosion in soils is an electrochemical process that is influenced by factors such as water content, degree of aeration or redox potential, pH, soil resistivity, soluble ionic species, and microbiological activity (Roberge 2000). Corrosion in soil is generally increased by higher aeration and redox potential as oxygen participates in the cathodic reaction. Within the pH range from 7 to 8, pH is not considered to be a dominant variable affecting corrosion rate. Elevated salt concentration enhances corrosion by decreasing the resistivity of the soil and increasing ionic current flow associated with soil corrosion. Chloride ions are particularly harmful as they participate directly in the anodic dissolution of metals and cause pitting in stainless steel (Roberge 2000).

Between 1984 and 1993 magnesium chloride brine was applied to unpaved roadways at a radioactive waste Subsurface Disposal Area (SDA) at the Idaho National Engineering and Environmental Laboratory (INEEL) to stabilize the roads. The distribution and persistence of chloride ions and other dissolved salts from the brine is of concern because of the potential to accelerate the release of radionuclides from buried metal containers and activated metals. Corrosion of beryllium reflector blocks is of particular concern because of the release of carbon-14 and tritium contained in the metal (Ritter and McElroy 1999).

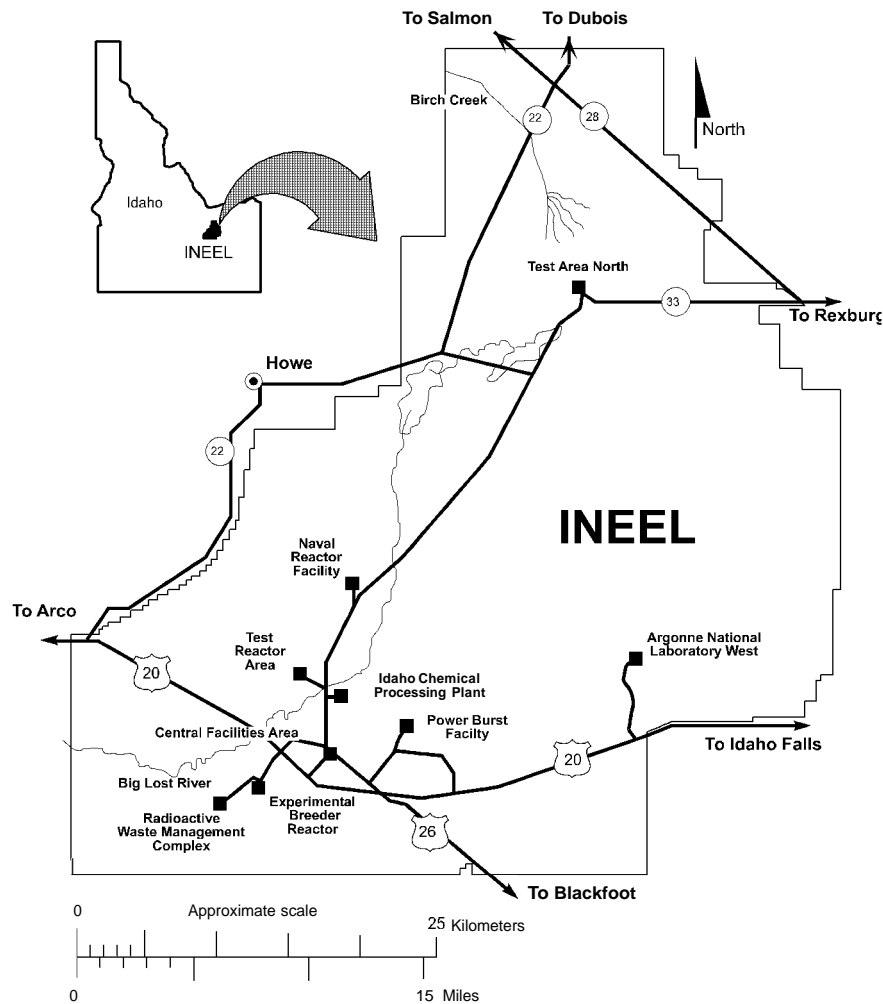
The objective of this project is to investigate the possibility that magnesium chloride brine applied to the subsurface disposal area came into contact with buried radioactive wastes. Direct sampling of waste and pore water within the waste is not possible. Therefore, indirect observations and measurements must be used to evaluate the likelihood that brine has migrated into waste. The approach taken to study the fate of magnesium chloride brine involves three steps:

- Where and how much brine was applied to roads in the SDA?
- How far and how fast did brine move in pore water and surficial sediments?
- Is the brine being flushed from the surficial sediments?

From these observations, we will evaluate whether chloride may have come into contact with buried waste and whether chloride is persistent in the SDA.

2. SITE DESCRIPTION

The INEEL is a U. S. Department of Energy-managed reservation that has historically been devoted to energy research and related activities. More nuclear reactors, and a wider variety of reactor types, have been built at the INEEL than at any other location in the world. The INEEL is located in southeastern Idaho (Figure 1) and occupies 890 mi² in the northeastern region of the Snake River Plain. The surface of the INEEL is a relatively flat, semiarid, sagebrush desert. Predominant relief is manifested as volcanic buttes jutting up from the desert floor. Elevations on the INEEL range from 4,790 ft in the south to 5,913 ft in the northeast, with an average elevation of 5,000 ft above sea level (Irving 1993). Mountain ranges bordering the INEEL on the north and west are the Lost River Range, the Lemhi Range, and the Beaverhead Mountains of the Bitterroot Range.



WAG7JB97-004

Figure 1. Map of showing the location of the INEEL in southeastern Idaho and the location of the Radioactive Waste Management Complex.

The Radioactive Waste Management Complex (RWMC) consists of three separate areas: The Subsurface Disposal Area (SDA), the Transuranic Storage Area (TSA), and an administrative support area. The SDA was opened in 1952 for shallow land disposal of solid, radioactive waste generated from

experiments associated with development of nuclear power reactors, reprocessing of spent nuclear fuel, and nuclear weapons construction. The SDA area is 97 acres. In the SDA, waste is buried in cardboard boxes, plywood boxes, carbon steel drums, or, for bulky items, placed directly into pits or trenches (Holdren et al. 2002). The SDA is still open for disposal of low-level radioactive waste. The TSA was added to the RWMC in 1970 to store transuranic waste aboveground. The TSA area is 58 acres. Contact-handled transuranic waste stored in the TSA is being processed and shipped to the Waste Isolation Pilot Plant in New Mexico.

2.1 Meteorology and Climatology

Meteorological and climatological data for the INEEL and the surrounding region are collected and compiled from meteorological stations operated by the National Oceanic and Atmospheric Administration field office in Idaho Falls, ID (Clawson, Start, and Ricks 1989). The Snake River Plain is classified as arid to semiarid with average annual precipitation at the INEEL of 8.7 in. Precipitation is highest in May and June and lowest in July. Normal winter snowfall occurs from November through April and ranges from a low of 6.8 in. per year to a high of 59.7 in. per year with an annual average of 27.6 in. The potential annual evaporation from saturated ground surface at the INEEL is 43 in. About 80% of this evaporation occurs between May and October. During the coldest months, December through February, evaporation is low and may be insignificant. Actual evaporation rates are much lower than potential rates because the ground surface is rarely saturated. Evapotranspiration by the sparse native vegetation of the Snake River Plain is estimated to be 6–9 in. per year, or four to six times less than the potential evaporation. Periods when the greatest quantity of precipitation water is available for infiltration (late winter to spring) coincide with periods of relatively low evapotranspiration rates (EG&G 1981).

2.2 Geology

The INEEL is located on the Eastern Snake River Plain, a northeast trending structural basin about 200 mi long and 50–70 mi wide in southeastern Idaho. The plain is underlain by a layered sequence of Tertiary and Quaternary volcanic rocks and sedimentary deposits (Anderson and Lewis, 1989). Volcanic rocks in this sequence consist of basaltic lava flows and cinder beds. During periods of volcanic quiescence, fluvial, lacustrine, and eolian sediments were deposited. Alternating periods of volcanic activity and sedimentary deposition have accumulated into a complex sequence of layers (Figure 2). Anderson and Lewis (1989) defined 10 basalt flow groups and seven major sedimentary interbeds underlying the SDA.

The SDA was constructed in unconsolidated sediments in a natural topographic depression surrounded by basalt lava flows. Undisturbed surficial sediments at the SDA range in thickness from 2 to 25 ft and consist primarily of fine-grained playa and alluvial material (Kuntz et al. 1994; Anderson, Liszewski, and Ackerman 1996). Irregularities in sediment thickness generally reflect the undulating surface of underlying basalt flows. Many physical features are common within the sediment stratigraphy of the SDA area such as pebble layers, freeze-thaw textures, glacial loess deposits, and platy caliche horizons. Surface soil in the SDA has been significantly disturbed, with additional backfill brought in from nearby playas to fill in subsidence depressions and recontour the surface for runoff control.

Basalt flows at the SDA occur as layered flow groups. Anderson and Lewis (1989) report a maximum measured flow thickness of 40 ft with flow thicknesses typically ranging from 5 to 17 ft. Basalt flows in the surface and subsurface at the INEEL were formed by three general methods of plains-style volcanism: low-relief shield volcanoes, fissure-fed flows, and major tube-fed flows (Greely 1982; Hackett and Smith 1992). The very low shield volcanoes, with slopes of about 1 degree, formed in an overlapping manner. This overlapping and coalescing of flows is characteristic of the low surface relief on the eastern Snake River Plain (Greely 1982). Considerable variation in texture occurs within individual basalt flows. In general, the bases of basalt flows are glassy to fine-grained and minutely vesicular. Middle portions of basalt flows are typically coarser-grained with fewer vesicles than the top or bottom of the flow. Upper portions of flows are fine-grained and highly fractured with many vesicles. This pattern is the result of rapid cooling of the upper and lower surfaces with slower cooling of the interior of the basalt flow. The massive interiors of basalt flows are typically jointed with vertical joints in a hexagonal pattern formed during cooling.

The interbeds consist of generally unconsolidated sediments, cinders, and breccia. Using the Anderson and Lewis (1989) nomenclature, the interbeds are called the A-B, B-C, and C-D sedimentary layers, so named for the basalt flow groups (i.e., A, B, C, and D) that bound the layers above and below. The three uppermost sedimentary layers also are commonly referred to as the 30-, 110-, and 240-ft interbeds. The C-D interbed is by far the most continuous. However, each of the interbeds contains known gaps. The A-B interbed is very discontinuous and generally exists only beneath the northern half of the SDA.

Physical, chemical, and mineralogical characteristics of the RWMC area sediment are detailed in Dechert, McDaniel, and Falen (1994) and McDaniel (1991). Generally, the sediment mantling the landscape surrounding the RWMC was deposited as loess during the Pinedale glaciation period and mixed with eolian sand and slope wash in lower areas of the basin. Sediment from the RWMC typically has high clay (approximately 36%) and high silt (approximately 56%) content (Chatwin et al. 1992). Generally, the sediment has moderate water-holding capacity, though some areas of the RWMC have shallow sediment with low water-holding capacity (Bowman et al. 1984). Some RWMC sediment also may be derived from historic stream deposits from the Big Lost River.

The mineralogy of the surficial sediments and sedimentary interbeds has been studied by the U. S. Geological Survey (Bartholomay, et al. 1989; Bartholomay 1990). The sediment has a nominal mineralogy of 35% quartz, 30% feldspar, 10% pyroxene, 4% calcite, 2% dolomite, and 19% clays. Predominant clay minerals are illite, smectite, and kaolinite. The mineralogy of sediments at the SDA correlate with minerals from source areas in the adjoining mountains. Sediments in different interbeds are mineralogically very similar. This evidence indicates a fairly uniform depositional process over time, which has lead to a similar mineralogy in the sediments (Bartholomay 1990).

2.3 Hydrology

2.3.1 Surface Water Hydrology

The SDA is located within a natural topographic depression with no permanent surface water features. However, the local depression tends to hold precipitation and collect additional runoff from the surrounding slopes. Surface water within the SDA and the surrounding local area does not reach the Big Lost River (Keck 1995). Surface water either eventually evaporates or infiltrates through the vadose zone to the underlying aquifer.

Historically, the SDA has been flooded by local runoff at least three times because of rapid snowmelt combined with rain and frozen ground. Dikes and drainage channels were constructed around

the perimeter of the SDA in 1962 in response to the first flooding event. Following a second flood in 1969, the height of the dike was increased and the drainage channel around the perimeter was enlarged. The dike was breached by accumulated snowmelt in 1982, resulting in a third inundation of open pits within the SDA. Significant flood-control improvements were made between 1985–1987 in response to this flooding (Holdren et al. 2002). These improvements included increasing the height and breadth of the dike, deepening and widening the drainage channel, and contouring to eliminate formation of surface ponds and to route runoff to drainage channels. Up to five ft of playa sediment was added to the surface of the SDA, in places, to route runoff to drainage channels. Localized runoff from surrounding slopes is now prevented from entering the SDA by the perimeter drainage channel and dike surrounding the facility.

During spring snowmelt, meltwater and precipitation falling on the SDA can redistribute to low areas, typically in the ditches along the roads. Figure 3 shows the distribution of meltwater at the SDA in February 1995. The depth of ponds in the southern half of the SDA was generally a few inches, while those along the central east-west axis of the SDA were generally 1 ft deep or more (Bishop 1998).

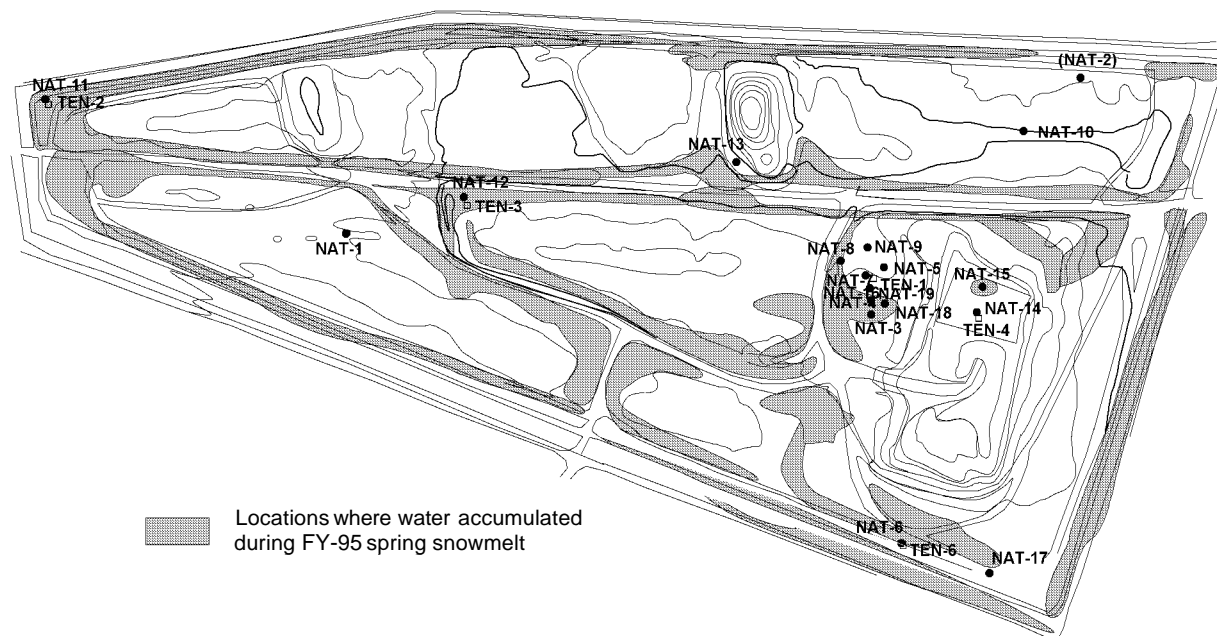


Figure 3. Map of the Subsurface Disposal Area showing the distribution of ponded water from snow-melt in the Spring of 1995 (Bishop 1998).

2.3.2 Vadose Zone Hydrology

The vadose zone (defined as the unsaturated region between land surface and an underlying aquifer) consists of surficial sediments, relatively thin horizontal basalt flows, and occasional interbedded sediments (Figure 2). Approximately 90% of the vadose zone thickness is composed of sequences of interfingering basalt flows. These sequences are characterized by large void spaces resulting from fissures, rubble zones, lava tubes, undulatory basalt-flow surfaces, and fractures. Sedimentary interbeds found in the vadose zone consist of sands, silts, and clays and are generally thin and discontinuous. Sediments may be compacted because of subsequent overburden pressures.

The vadose zone thickness near the SDA, based on recent water-level measurements, is approximately 590 to 610 ft. Rates of moisture movement in sediments and basalt under varying moisture

conditions have been quantified near the SDA. These quantified rates vary widely and depend on the location, material type, and timing of infiltration at the surface. Bishop (1998) reported wide variations in net drainage from surficial sediments into the underlying basalt over a 3-year period. Net drainage, or recharge, was measured at neutron-probe access tube locations in the SDA, and ranged from a high of 19.5 in./year to less than 0.1 in/year. The wide range in recharge was attributed to yearly changes in accumulated snowfall, spring drainage patterns of runoff and ponding, and proximity of the measurement locations to areas of runoff or ponding. During the aquifer pumping and infiltration test in the summer of 1994 (Porro and Bishop 1995), a moisture movement rate of 16 ft/day was measured from land surface to a depth of 180 ft through the fractured basalt medium. The infiltration test was conducted approximately 1.3 mi south of the SDA.

2.3.3 Perched Water

Perched water at the INEEL forms when a layer of dense basalt or fine sedimentary materials occurs with a hydraulic conductivity that is sufficiently low that downward movement of infiltrating water is restricted. Once perched water develops, lateral movement of the water can occur, perhaps up to hundreds of feet. When perched water accumulates, the hydraulic pressure head increases until the water can flow through the less permeable perching layer. If another restrictive zone is encountered, perching may again occur. The process can continue, forming several perched water bodies between the land surface and water table. The volume of water contained in perched bodies fluctuates with the amount of recharge available from precipitation, surface water, and anthropic sources such as infiltration ponds. Perched water zones tend to slow the downward migration of percolating fluids that may be flowing rapidly under transient near-saturated conditions through the vadose zone.

Perched water is transitory beneath the SDA but has been detected in 11 boreholes at various times (Hubbell 1993, 1995; McElroy 1996). Typically, perched water wells are dry or contain so little water that the volume collected for analysis is limited. Perched water bodies have been identified at two depth intervals at the SDA, at depths of approximately 80–90 ft and 200–220 ft, corresponding to the sedimentary B-C and C-D interbeds, respectively (Figure 2). Perched water typically occurs in fractured basalt above the interbeds. Sources of perched water at the SDA may be: (a) surficial infiltration, (b) water moving laterally from the spreading areas of the Big Lost River, or (c) a combination of sources. A tracer test conducted by the U.S. Geological Survey confirmed that at least some of the perched water in Well USGS 92 beneath the SDA originated from the spreading areas (Nimmo et al. 2002).

3. MAGNESIUM CHLORIDE BRINE TREATMENTS

In the past, operation of heavy equipment on unpaved roads at the SDA generated large quantities of airborne dust that limited visibility. To control the dust, a chemical solution of magnesium chloride brine was experimentally applied to 2.5 mi of dirt roads at and around the SDA in August 1984 (INEL News, September 18, 1984). The treatment met the objectives of controlling dust, and the brine was subsequently reapplied in 1985, 1992, and 1993. The first objective of this report is to document where and how much brine was applied to roads in the SDA.

3.1 Brine Chemistry

The chemical used on the roads at SDA is a magnesium chloride brine solution. Although it contains several other salts, the main components are magnesium chloride (MgCl_2) and water. Magnesium chloride is a hygroscopic chemical. Hygroscopicity is the property possessed by some chemicals that allows them to absorb moisture from the air. By adsorbing moisture from the air, the magnesium chloride keeps the road surface moist, preventing dust. The chemical composition of the brine applied to SDA roads, reported by the manufacturer, is shown in Table 1. The table shows that the weight ratio of the main brine components consists of 29–35% magnesium chloride and 62–72% water (H_2O).

Table 1. Chemical composition of magnesium chloride brine applied to SDA.

Component	Typical Weight Percent	Estimated mg/L
Magnesium	7.1–9.2	114,530
Calcium	See note	120
Sodium	0.2–1.0	11,200
Potassium	0.1–0.8	8,400
Lithium	0.1–0.2	2,500
Chloride	21–27	356,240
Sulfate	1.2–2.0	26,300
Bromide	0.1–0.2	765
Bicarbonate	See note	384

Note: No calcium or bicarbonate are given for the brine. These numbers are calculated assuming the brine is saturated with respect to calcite at atmospheric P_{CO_2} . The brine has a density of 11 lbs/gal.

3.2 Brine Application

Applying magnesium chloride brine to stabilize roads, control fugitive dust emissions, and to minimize suspended solids contamination of storm-water runoff is a well-accepted practice (Hansen 1982; Skorseth 2000). Road surface preparation is important for the brine treatment to be effective. The first step in surface preparation at the SDA was to grade and smooth the road surface to set the grade and remove potholes, wash boarding, and furrowing. In addition, curves in the roads were banked to prevent shearing caused by vehicular traffic. A main purpose of this roadwork was to reduce brine ponding on the road surface and to facilitate uniform brine distribution. Good drainage from the road surface was necessary before the brine residues could combine to form a harder road surface. Before application, the roads were scarified and prewetted to a depth of 5 in. Brine was then applied at the recommended rate of 0.5 gal/yd². One to four additional applications of water were necessary to aid in the hardening process after the brine was applied. When brine is applied properly, the salt is tightly bound into the roadbed material, and forms a dense, low permeability layer.

The choice of roads receiving brine varied from application to application. Figure 4, a map of the SDA, shows roads where the brine was applied in August 1984, May 1985, and July 1992. Dust and erosion suppressant was applied again in 1993. A map for the 1993 brine application was not found, but a requisition for the application subcontract was found. It is assumed that the 1993 application was made in generally the same areas as the previous applications.

Brine was purchased from Great Salt Lake Minerals or Kaiser Chemicals. Standard practice for road stabilization with brine is to apply 0.5 gal/yd² (Hansen, 1982). From the application areas shown in Figure 4, the amount of brine applied to roads inside and around the SDA can be estimated. Based on language in the purchase requisition for the 1993 brine application, roads were assumed to be 30 ft wide, and brine application was at 0.5 gal/yd². Results of the calculations are shown in Table 2. The 1993 contract for brine application called for 285 tons of brine to cover 6 mi of road, 30 ft wide (Schless requisition for the May 1993 application, 1992). Based on earlier estimates of the amount of brine applied in and around the SDA, a significant portion of the 1993 application must have included dirt roads away from the SDA. From the application maps, the total amount of brine applied inside and immediately around the SDA is estimated to be 660 tons. About 27% of the brine by weight is chloride ion. Based on the brine application amounts estimated in Table 2, 178 tons of chloride are estimated to have been added to SDA roads between 1984 and 1993.

The first step to evaluating whether brine application may contribute to corrosion of waste in pits and trenches is to examine the relation between the roads where brine was applied, and the locations of pits and trenches. Environmental impacts from road-salt applications have mainly been evaluated for salts used in deicing applications. Little is known about the impacts of brine used for road stabilization. The environmental impacts of road salt mainly occur within a few yards of the roadway, or occur along drainage channels leading away from the road (Lewis 1999; Wegner and Yaggi 2001). Most of the brine impacts, therefore, are expected to be under the roads and along the drainage ditches beside the roads.

The locations of brine application and the locations of pits and trenches are shown in Figure 4. The roads generally do not cross pits and trenches, with four notable exceptions. Areas where roads treated with brine directly cross pits or trenches are:

- East of Pit 15 over trenches 50, 52, 54, 56, and 57
- South of Pit 20 over soil vault row (SVR) 12
- South of Pit 13 over trenches 12, 14, 16, 19, and 40, 42, 45, 47, 49, 51, 53, 55
- West of Pits 4 and 10 over trenches 2, 3, 4, 6, 8, 10, and SVRs 9 and 10.

In these four areas, brine leaching from the roadbed, or from drainage ditches along the side of the road, would move directly down into buried waste. Brine-treated roads are in close proximity to SVRs along the main haul road south of Pit 3 and Pad A and immediately south of Pit 20 (Figure 4). At the west end of the SDA, the main haul road is bounded on the north by Pit 2, and on the south by trenches. Most of the roads where brine was applied are immediately adjacent to waste, so with minimal lateral spreading, brine could contact waste. Figure 4 also shows the locations where activated beryllium blocks are buried. East of Pit 15, the road where brine was applied runs directly over one of the beryllium disposal locations.

From the maps showing the locations where brine was applied, there are locations where brine was applied directly over buried waste, and contact between the waste and brine is probable. In many other locations, roads run adjacent to waste within a few feet. Depending on the ability of the brine to spread laterally in the surficial sediments, opportunities exist for brine to contact waste in pits, trenches, and SVRs.

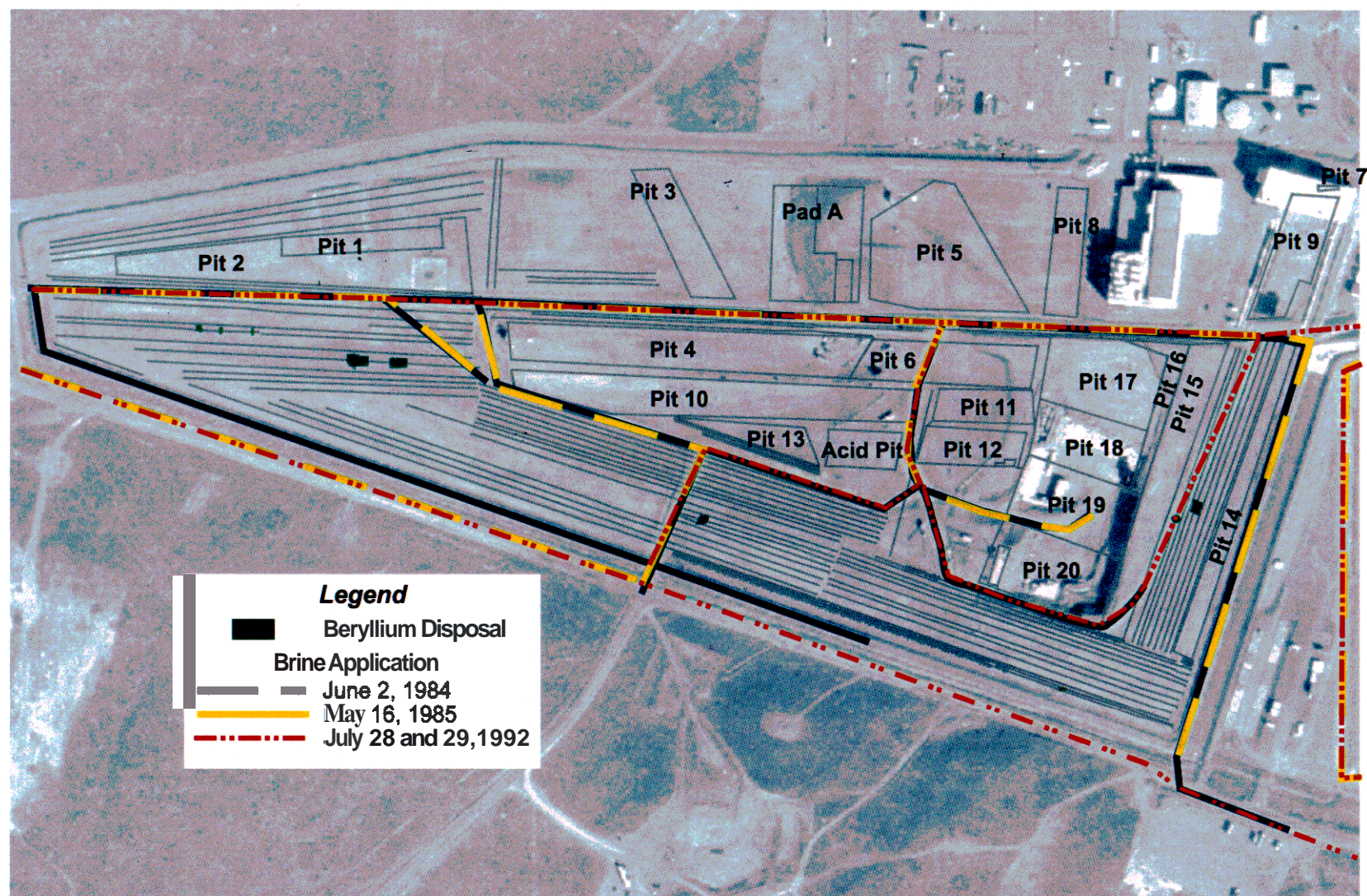


Figure 4. Map showing the SDA roads that were treated with *dust* suppressant in 1984, 1985, and 1992. No map is available for the 1993 brine treatment. The map also shows the locations of pits and trenches in the SDA, and shows that brine was applied directly over some of the waste disposal locations.

Table 2. Estimates of the total tons of brine applied to roads in and around the SDA.

Year	Inside the SDA (tons of brine)	Around the SDA (tons of brine)	Total (tons of brine)	Other Total Estimate (tons of brine)
1984	94.25	16.31	110.56	119.02 ^a
1985	48.53	52.21	100.74	—
1992	60.53	163.10	223.62	—
1993	60.53 ^c	163.10 ^c	223.62 ^c	258.53 ^b
Total	263.84	394.71	658.54	—

a. Estimated from 2.5 mi of roads, 30 ft wide, 0.5 lbs/yd² from the 1984 newspaper article.

b. Taken from 1993 purchase requisition for 258 tons of brine.

c. Assumed to cover the same area as the 1992 application.

4. BRINE IN VADOSE ZONE PORE WATER

The second objective of this report is to document the distribution of chloride in the pore waters at the SDA, and evaluate the amount of lateral spread of chloride in the subsurface. This section discusses the vadose zone monitoring network in place at the SDA and summarizes the water chemistry data collected from that network. Spatial distribution, as well as changes with time, are presented.

4.1 Vadose Zone Monitoring Network

Suction lysimeters are designed to collect moisture from unsaturated sediment by creating a vacuum inside the lysimeter and drawing moisture through a porous material into the lysimeter where it can be collected for analysis. The majority of the lysimeters at the SDA have either ceramic or stainless steel cups. Four lysimeters with teflon cups also were installed because of the concern that radionuclides may sorb on ceramic cups (Hubbell et al. 1985), which could cause biased, low-detection results. The lysimeters with teflon cups were never successful in collecting sediment-water samples because the low air-entry pressure prevented the use of a vacuum that was high enough to extract water from the SDA sediment. An inventory of lysimeters installed at the SDA is given in Appendix A. The locations of wells containing lysimeters installed at the SDA are shown in Figure 5.

Installation of lysimeters at the SDA began in 1985 to determine solution chemistry and to define radionuclide migration in the vadose zone (Hubbell et al. 1985; Rawson et al. 1991). From 1985 through 1987, 32 suction lysimeters were installed in surficial sediments in and around the SDA, and seven deep lysimeters were installed in sedimentary interbeds (Hubbell et al. 1985, 1987; Laney et al. 1988). Because multiple lysimeters were installed in boreholes, the naming nomenclature for the lysimeters relies on individual lysimeter numbers. Shallow lysimeters were installed in auger holes with a silica flour slurry surrounding the lysimeter cup. A 2- to 3-in. layer of bentonite was placed on top of the silica flour as a moisture seal and native sediments were used to backfill the borehole. Deep lysimeters in the B-C and C-D interbeds were installed in a silica flour slurry, and bentonite was used to seal between instrument installations in the same borehole. A silica flour slurry with a 10-mg/L potassium bromide tracer was used for lysimeters installed in 1986 and 1987 to determine when valid samples were collected. The presence of the potassium bromide tracer in sample analysis would indicate that water applied during instrument installation is still affecting sample results, whereas absence of the tracer would indicate that the sample is representative of local sediment moisture.

As part of remediation and monitoring activities for Pad A, two lysimeters were installed in December 1994. Lysimeter L33 was installed at a depth of 10 ft below the surface of Pad A on the north side in Borehole PA-03. Pad A is an aboveground disposal area located on an asphalt pad. However, well logs indicate that drillers did not encounter the asphalt pad when augering Borehole PA-03; therefore, either the asphalt pad does not extend as far as Borehole PA-03, or the lysimeter is located in cover material above the asphalt pad. Lysimeter L34 was installed in a horizontal borehole under the asphalt at Pad A in Borehole PA-04. Lysimeter L34 is located near the center of Pad A, approximately 165 ft northeast of the Borehole PA-04 wellhead. Both lysimeters were installed in silica flour, with bentonite used to seal the silica flour layer.

Suction Lysimeters L40 and L41 were installed in 1994 to collect water samples near buried beryllium blocks near the west end of SVR-20 to validate calculated beryllium corrosion and radionuclide release rates used in low-level waste operations performance assessments (Case et al. 2000). Lysimeter cups were placed in native fill material with a layer of sand above and below the lysimeter, and the borehole was backfilled with bentonite. Several attempts were made to collect a sample from L40, but a sufficient vacuum to collect a sample could not be maintained. However, the deeper lysimeter, L41, yielded sufficient sample volume to analyze for chloride, C-14, and tritium (Ritter and McElroy 1999).

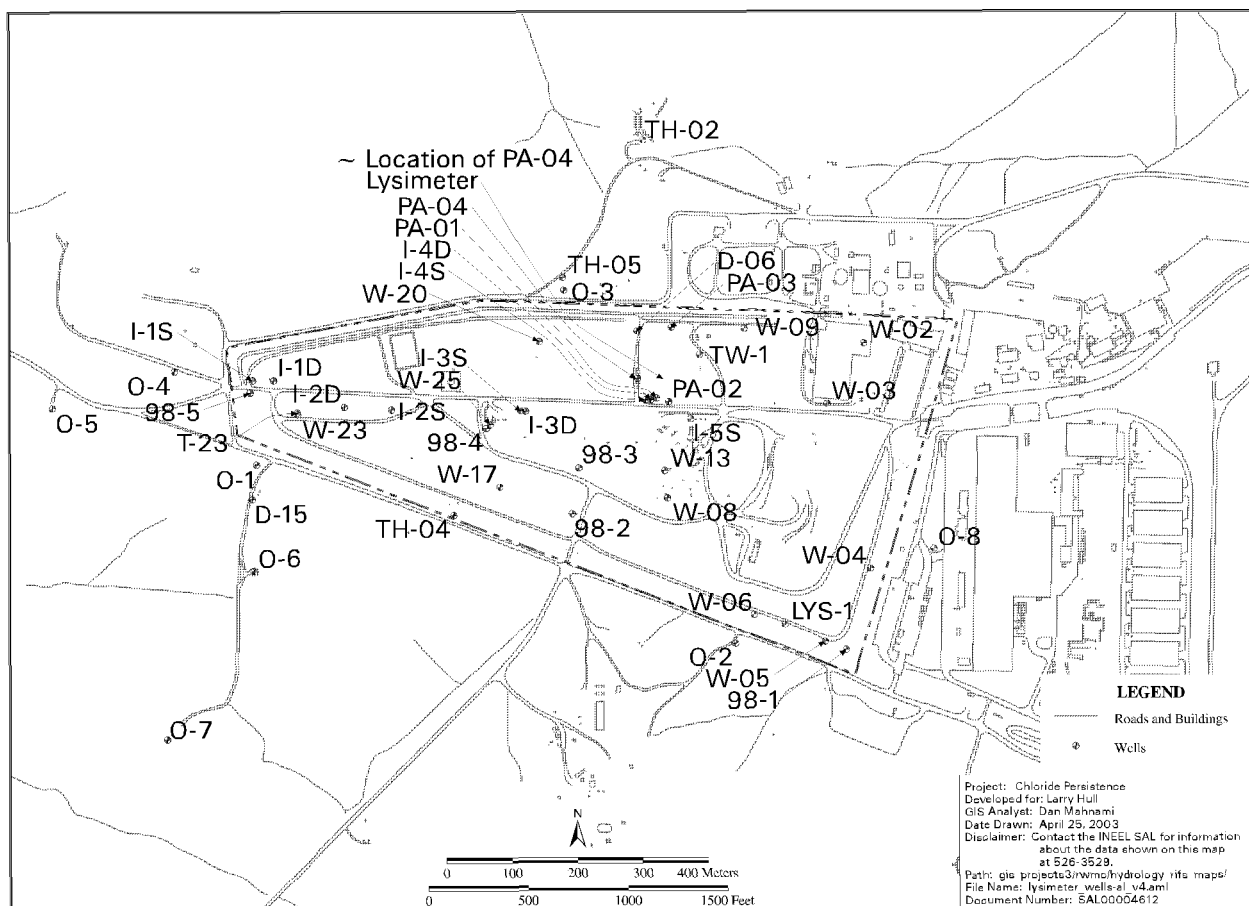


Figure 5. Locations of wells where suction lysimeters are installed at the Subsurface Disposal Area.

Five lysimeters, L35 through L39, were installed in surficial sediments in the **SDA** in 1998 to assess magnesium chloride migration in sediment at the SDA. Each of these lysimeters was installed as close as possible to the sediment-basalt interface. A sediment slurry was placed around the porous ceramic cup, native sediment was used to backfill the borehole, and a 1-ft layer of bentonite was placed 2 ft above the instrument to serve as a barrier to downhole water movement.

From November 1999 through March 2000, 22 deep lysimeters, DL08 through DL29, were installed inside and outside the **SDA**. The porous cups on these lysimeters are stainless steel with a -600 cm of water air entry pressure. Installation was similar to the procedure described above with silica flour slurry between layers of bentonite.

Very small volumes of sediment moisture, typically 0 to 200 mL, are usually obtained from lysimeters, and 50 mL of that total volume is generally allotted for each separate analysis. The detection limits vary with the sample volume available for analysis. Detection limits increase (i.e., are less sensitive) as sample volumes decrease because of the difficulty associated with precision measurement of small amounts of sample matrix. When the sediment is relatively dry, a sediment moisture sample cannot be collected from the lysimeter. Analyses are prioritized to obtain the most essential data first.

Perched water is present in isolated lenses above the sediments comprising the B-C and C-D interbeds. Samples from the water perched above the **C-D** interbed are obtained with a bailer from Wells USGS-92 and 8802D. Well USGS-92 was installed in 1972, Well 8802D in 1988. These perched water wells have slow

recharge rates and thin depths of water, often limiting the volume of water sample that can be collected in the bailer. Generally, samples can be collected at Well USGS-92, but success is sporadic at Well 8802D.

4.2 Vadose Zone Pore-Water Chemistry

Suction lysimeters are sampled to monitor for migration of contaminants of concern and for major water chemistry parameters. This section focuses on the major ion chemistry of the waters that relates to the distribution and persistence of brine. Major ion chemistry includes the cations calcium, magnesium, sodium and potassium; and the anions bicarbonate, sulfate, chloride, nitrate-N, and bromide. From the measurement of major cations and anions, water types can be identified, waters can be linked back to possible sources, and trends can be established. The vadose zone at the SDA has been divided into three zones:

- Shallow < 35 ft,
- Intermediate 35 to 140 ft,
- Deep > 140 ft.

Pore water chemistry data are discussed following this division of the vadose zone.

4.2.1 Shallow Vadose Zone

The shallow vadose zone consists of the surficial sediment to depths less than 35 ft below land surface. This zone corresponds to the layer of surficial sediment and extends from land surface to the top of the youngest basalt flow. This is also the layer in which the waste is buried. The lysimeters are installed around and near the waste, but none of these lysimeters is installed in or under the buried waste.

There are 41 suction lysimeters installed in the shallow vadose zone. Thirty-two were installed in 1985 and 1986, and nine additional in 1994 and 1998 (Appendix A). The lysimeters in this zone have the longest history of sampling. Lysimeters were sampled a few times a year in 1986, 1987, and 1988. Few samples were collected between 1989 and 1998. Since 1998, sampling has resumed on a more regular basis. Analysis for major cations and anions are prioritized below analyses for contaminants of concern. As such, samples are gathered less frequently. The frequency of sampling can be deduced from Table 3. From the period before 1990, there were up to 166 samples, summed over all lysimeters, for many parameters. Since 1990, there have been a few, to a few dozen, samples. Detection limits for the pre and post 1990 sampling are very different, with more recent samples having detection limits about two orders of magnitude better than the earlier samples.

When a complete set of major cations and anions are quantified for a water sample, it is possible to identify trends and groupings of water samples that share common chemical attributes. A Piper diagram is a good way to illustrate these trends or clusters. The Piper diagram consists of two triangles and a diamond (Figure 6). The left triangle summarizes the cations, with one axis representing calcium, the second axis representing magnesium, and the third axis representing sodium plus potassium. Values are plotted as the percentage of the total in milliequivalents per liter. A sample that plots at one of the apexes of the triangle indicates that one particular ion dominates the water chemistry. Waters that plot toward the center of the triangle indicate mixtures of cations with about equal amounts of all cations. The anions from a water analysis are plotted in the right triangle, with the axes representing bicarbonate, chloride, and sulfate. A water sample has a point in each triangle. The cation and anion points are then projected into the central diamond, with a symbol plotted at the intersection of the two projections. The size of the symbol in the diamond portion of the Piper diagram in Figure 6 is proportional to the chloride

concentration in the sample, except for the symbol for brine, which would block out most of the diagram if plotted to scale. The symbols in the two triangles are not scaled to chloride concentration.

Table 3. Summary statistics for water samples collected from suction lysimeters in the shallow vadose zone at the SDA.

0 to 35 ft	Number of Samples			Detection Rates			Summary Statistics				
	Before	Since			Not		Average	Minimum	Maximum		
Analyte	1990	1990	Total	Detected	Detected	% detects	of detects	of detects	of detects	Units	
Bicarbonate	152	15	167	167	—	100%	623	87	1750	mg/L	
Bromide	66	58	124	109	15	88%	5.14	0.052	33	mg/L	
Calcium	166	27	193	193	—	100%	318	7.08	2540	mg/L	
Chloride	147	66	213	213	—	100%	1390	1.1	13600	mg/L	
Diss. Oxygen	9	—	9	9	—	100%	5.97	4.2	8.3	mg/L	
Fluoride	153	41	194	184	10	95%	1.06	0.18	5.5	mg/L	
Magnesium	166	27	193	193	—	100%	223	8.39	1900	mg/L	
Nitrate-N	10	110	120	118	2	98%	42.7	0.12	319	mg/L	
Nitrite-N		49	49	13	36	27%	0.661	0.1	5.33	mg/L	
pH (field)	88	11	99	99	—	100%	7.56	6.54	8.49	—	
pH (lab)	132	15	147	147	—	100%	7.77	6.9	8.58	—	
Phosphate	162	57	219	44	175	20%	1.14	0.068	8.29	mg/L	
Potassium	166	27	193	193	—	100%	7.88	1.19	75.4	mg/L	
SiO2	166	—	166	166	—	100%	78.9	66.08	101	mg/L	
Sodium	166	27	193	193	—	100%	762	8.03	4070	mg/L	
Sulfate	150	59	209	209	—	100%	617	15	2570	mg/L	
Temperature	97	13	110	110	—	100%	16	10.3	23.5	°C	

Chemical analyses from selected representative water samples from the shallow vadose zone are plotted in Figure 6 and provided in tabular form in Appendix B. Water samples are divided into three groups, the magnesium chloride brine (star), water samples from areas of the SDA contaminated by brine (square), and water samples from areas not contaminated by brine (circle). The anion compositions of the uncontaminated water samples show that bicarbonate is the predominant anion in many of the water samples. There are a number of samples, however, that include more sulfate than bicarbonate. The cations in uncontaminated waters plotted in Figure 6 fall along a line between a mixed water type (equal amounts of calcium, magnesium, and sodium) and waters high in sodium.

The composition of the brine plots at the magnesium apex of the cation triangle and the chloride apex of the anion triangle. As brine migrates into the vadose zone, it mixes with the native pore water. In the anion triangle, there is a gradual change in the ratios of the anions, with chloride dominating the anion composition of waters contaminated by brine (squares). The primary change in anion composition as the brine moves through the vadose zone is an increase in the ratio of sulfate to chloride. Mass balance calculations show that this results from the addition of sulfate ion. The cation composition of pore water samples contaminated by brine are very similar to the uncontaminated water samples.

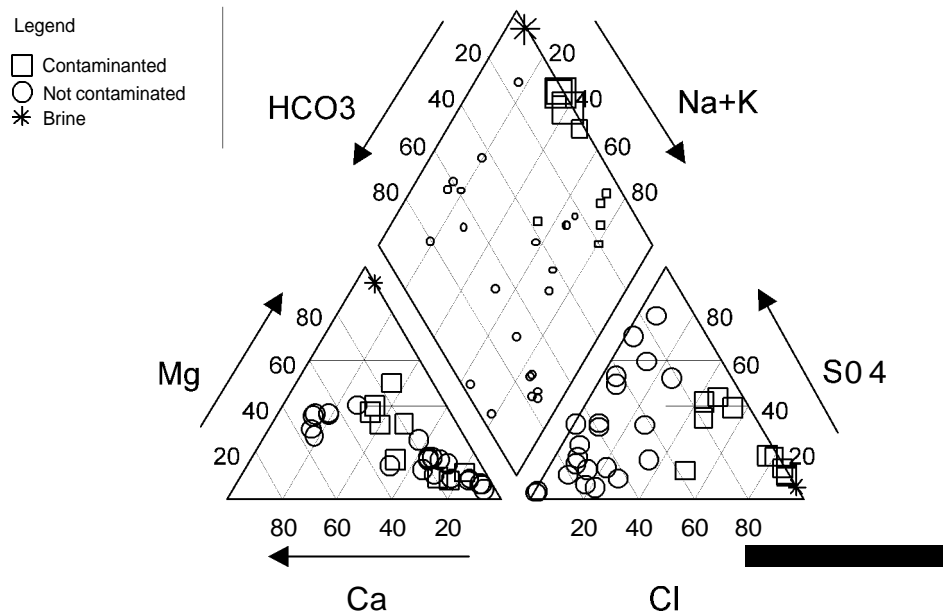


Figure 6. Piper diagram of waters in the shallow vadose zone. The star represents the magnesium chloride brine applied to roads, the squares are samples contaminated by brine, and the circles are the unaffected waters. Symbol size in the triangle is proportional to chloride concentration, except for the brine symbol.

4.2.1.1 Processes Controlling Wafer Chemistry. The brine contains chloride and bromide, both of which should be conservative species in vadose zone pore water (Hem 1992). To test this, a plot of bromide versus chloride was made (Figure 7). The brine is so much more concentrated than the pore water sampled at the SDA that the plot essentially consists of two points, the brine and all the other samples. Dilution is a linear process, and if water samples reflect dilution of the brine, they should plot on a straight line between these two points. A linear regression was performed to fit a line to the brine and the low-chloride pore waters from the SDA. This regression line is the dotted line in Figure 7. The bromide and chloride data were also plotted at a larger scale without the brine to show more detail for the pore water chemistry (Figure 8). A regression line was fit to the pore water chloride and bromide data excluding the brine composition. This regression line is the solid line in Figure 7 and Figure 8. The regression line for bromide versus chloride is essentially identical, whether brine is included or not. This linear relation between pore water chemistry and brine chemistry confirms that dilution of brine is responsible for the water samples from the SDA with elevated dissolved solids. Based on the chloride to bromide ratio, essentially all water samples from the SDA with 350 mg/L (10 meq/L) or more chloride have been contaminated by brine. With this information, the samples with brine contamination can be identified from the total chloride concentration and the chloride to bromide ratio. These samples are indicated with a square in Figure 6.

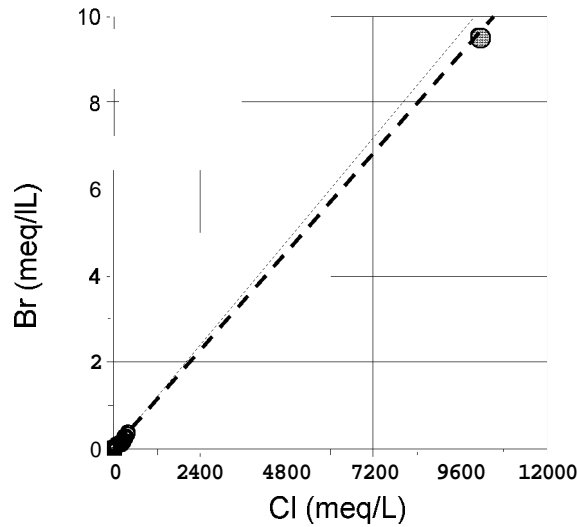


Figure 7. Correlation of chloride concentration to bromide concentration for water samples from the surficial sediment and for the brine applied to the roads.

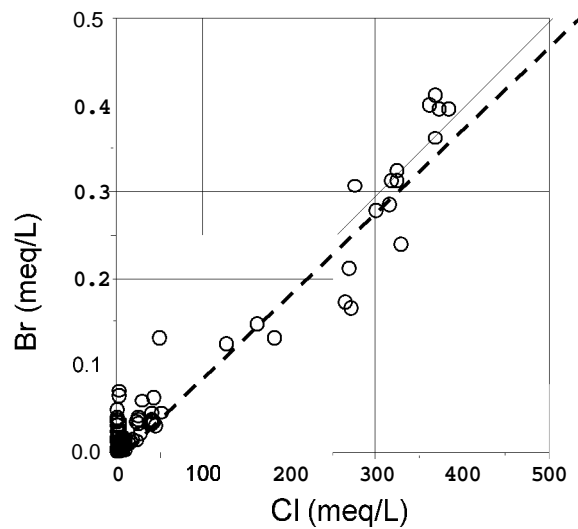


Figure 8. Correlation of chloride concentration to bromide concentration for water samples from the surficial sediment.

Bromide and chloride are shown to be conservative in pore water. Other solutes can then be compared to chloride to determine if they are conserved during dilution of brine or are added or removed from the water as the brine mixes with vadose zone pore water. Magnesium is plotted against chloride at two scales in Figure 9 and Figure 10. Figure 9 includes the composition of the brine. As with chloride, the magnesium in the brine is so much higher than the pore water that the plot appears as two points. Figure 10 focuses on the water samples from the lysimeters. Regression lines were fit with (dashed) and without (solid), including the brine composition. The two lines are very different, and the regression on the **SDA** pore water samples falls well below the brine regression line. Magnesium is not conserved during dilution of brine, but is removed from solution relative to chloride. In the Piper diagram (Figure 6), the large change in cation ratios between the brine and the rest of the pore-water samples in the **SDA** reflect this loss of magnesium relative to calcium and sodium.

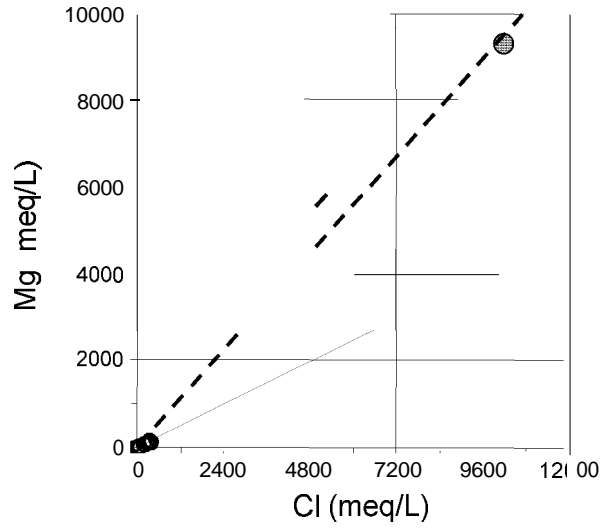


Figure 9. Correlation of chloride concentration to magnesium concentration for water samples from the surficial sediment and the brine applied to roads.

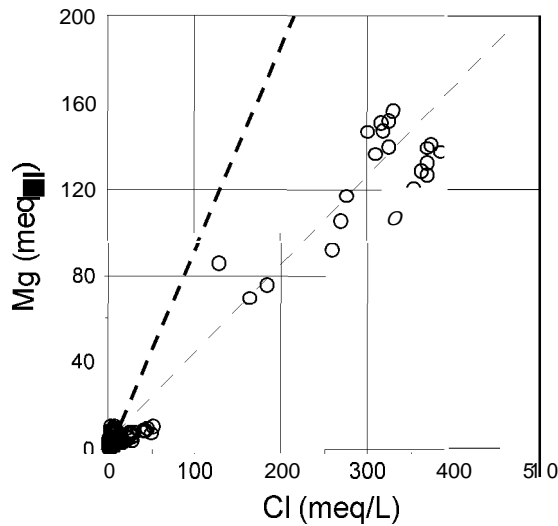


Figure 10. Correlation of chloride concentration to magnesium concentration for water samples from the surficial sediment.

A plot of sodium versus chloride shows that sodium concentrations in vadose zone pore water are higher than would be predicted by simple dilution of brine (Figure 11). There is a source of sodium to pore water in the vadose zone. This increase in sodium is also apparent in Figure 6 as most of the vadose zone pore waters plot in the sodium corner of the cation triangle. This high sodium is not all from the brine, however; another source of sodium must be present.

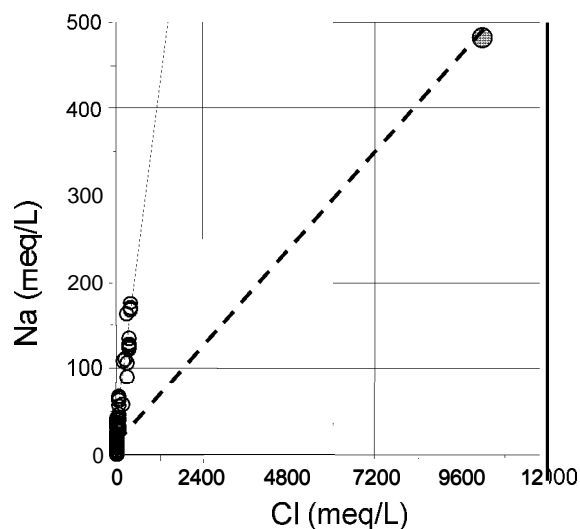


Figure 11. Correlation of chloride concentration to sodium concentration for water samples from the surficial sediment and the brine applied to roads.

Sulfate is another species that increases in shallow vadose zone pore water relative to the amount added by brine. In Figure 12 and 13, the slope of the correlation line that includes the brine (dashed line) is less than the slope of the line for the pore water samples. The increase in sulfate relative to chloride is also apparent in Figure 6 as the water samples affected by brine are arrayed along the extreme edge of the anion triangle between the brine and the sulfate apex of the triangle. As sulfate is added to the water, the fraction of total anion equivalents accounted for by sulfate increases.

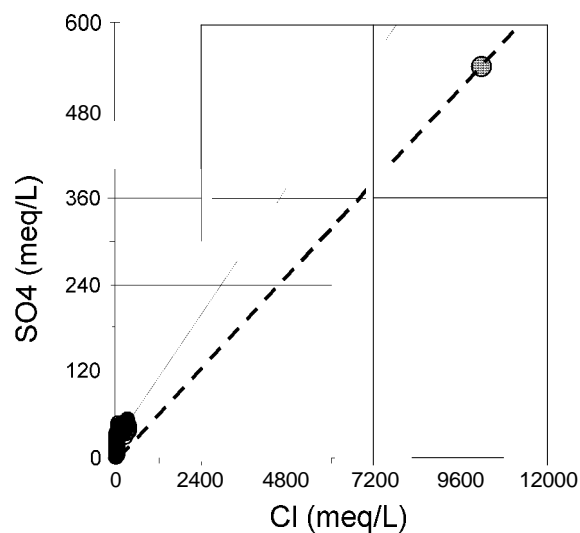


Figure 12. Correlation of chloride concentration to sulfate concentration for water samples from surficial sediment and the brine applied to the roads.

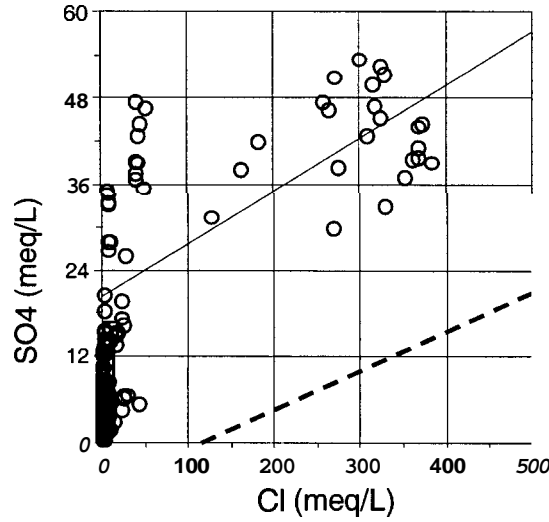


Figure 13. Correlation of chloride concentration to sulfate concentration for water samples from the surficial sediment.

4.2.1.2 Calculation of chemical mass balances. Changes in water chemistry can be quantified by calculating the expected water chemistry of sediment waters contaminated by brine and comparing it to the measured water chemistry. The calculation is based on the finding that chloride in the sediment water is conserved during brine dilution. The expected concentrations of the other ions are then calculated using the dilution factor calculated from chloride. The amount of ion added or removed from solution (A) is then calculated from the difference between the expected and measured concentration.

$$\Delta = S_s - \left(\frac{Cl_s}{Cl_B} \cdot S_B \right) \quad (1)$$

where:

- S_s = Measured solution concentration of chemical S (meq/L)
- Cl_s = Measured solution concentration of chloride (meq/L)
- Cl_B = Concentration of chloride in the brine (meq/L)
- S_B = Concentration of chemical S in the brine (meq/L)

The calculation is done in terms of milliequivalents/L. Milliequivalents are used to keep track of the total change in ionic charges. Because water must always be electrically neutral, the change in charges must always balance. For example, for every magnesium ion removed from solution (charge +2), an equivalent number of charges of another cation must be added to solution, or an equivalent number of charges of an anion must be removed from solution. Table 4 shows the results of this calculation.

The analyses show good charge balance. In the lower part of Table 4, the milliequivalents of each ion added and removed from solution relative to the amount of dilution are calculated. Chloride is zero (none added or removed), because chloride was used as the basis of the calculation to determine dilution. Both bromide and chloride should act conservatively in sediment water with a common source from the brine, and the zero differences calculated for bromide confirm that bromide is also conservative. The ions that are removed from solution relative to chloride are magnesium potassium, and lithium. Some ions

increase in concentration relative to chloride. These are calcium, sodium, bicarbonate, and sulfate. The excess cations and anions balance, keeping the water in electrical-charge balance (neutral).

The dilution graphs show that brine dilution is a significant control on major ion water chemistry in the shallow vadose zone at the SDA and that chloride and bromide are conserved during dilution. As the water mixes with native pore water in the sediments and becomes diluted, the water loses magnesium, potassium, and lithium, and gains calcium, sodium, sulfate, and a small amount of bicarbonate relative to chloride and bromide. The magnitude of the calculated changes in meq/L shown in Table 4 show that there are very large changes in the cation composition of the water, and relatively small changes in the anion composition. For example, for lysimeter L02, there are 248 meq/L of cations removed from solution and 275 meq/L of cations added to solution, while only 27 meq/L of anions are gained. This suggests that there are significant cation processes taking place in the water without the involvement of anions. This imbalance suggests that cation exchange is the most important process occurring during dilution.

Sodium salts are generally very soluble, and it is not likely that there are soluble sodium salts in the shallow vadose zone. A more likely source of sodium is ion exchange sites on clays. Magnesium in the brine exchanges for sodium ion on clays, removing magnesium from solution and increasing the sodium concentration. Ion exchange can also account for the fairly consistent ratio of calcium to magnesium in solution. The net effect of these trends on the cation composition of shallow vadose zone pore water can be seen in the Piper diagram Figure 14.

Table 4. Calculation of ion gains and losses relative to chloride from the original brine. Concentrations in meq/L.

In Lysimeters	Brine	L02	L25	L26	L08	L09
Ca	6.02	124	102	42.6	22.1	2.1
Mg	9,544	138	140	72	9.5	3.68
Na	487	170	128	111.6	64	43
K	216	0.68	0.382	0.282	0.268	0.2
Li	361	0.014	0.019	0.015	0.009	0.014
HC03	6.26	4.9	3.11	4.1	7.54	17.5
SO4	549	43.5	52	42	44.62	15.42
Cl	10,049	384	315	181	43.16	16.6
Br	10	0.395	0.325	0.149	0.036	0.015
meq/L imbalance	-0.24	-0.015	0.097	-0.657	0.572	-0.455
Calculated gain / loss	Brine	L02	L25	L26	108	109
Ca	0	123.77	101.81	42.49	22.07	2.09
Mg	0	-226.7	-159.2	-99.9	-31.5	-12.1
Na	0	151.39	112.73	102.83	61.91	42.20
K	0	-7.57	-6.39	-3.61	-0.66	-0.16
Li	0	-13.78	-11.3	-6.49	-1.54	-0.58
HC03	0	4.66	2.91	3.99	7.51	17.49
SO4	0	22.52	34.79	32.11	42.26	14.51
Cl	0	0.00	0.00	0.00	0.00	0.00
Br	0	0.01	0.01	-0.03	0.01	0.00
Excess cation meq/L		27.10	37.69	35.32	50.29	31.46
Excess anion meq/L		27.19	37.72	36.07	49.77	32.00

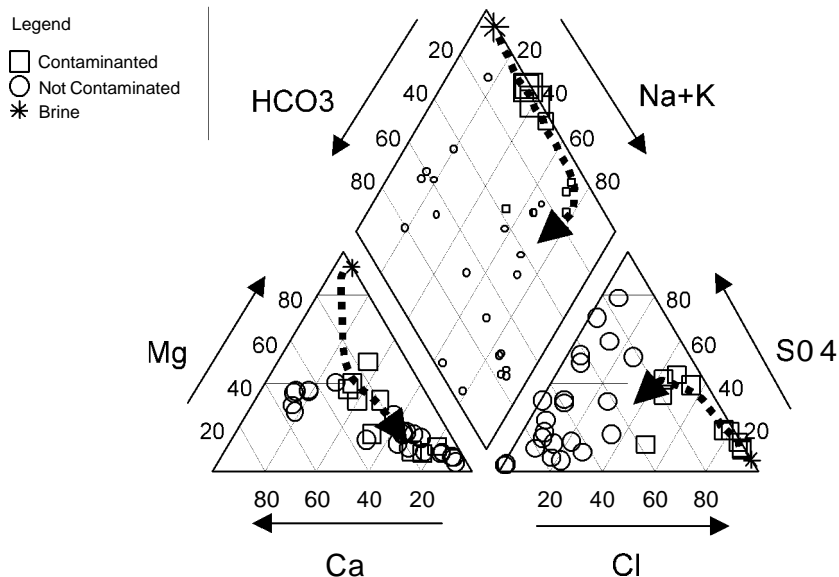
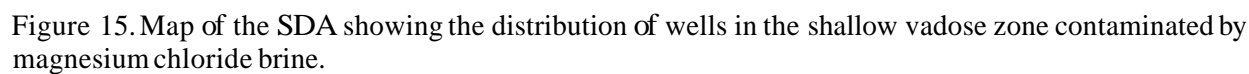


Figure 14. Piper plot of water chemistry in the shallow vadose zone showing the evolution of water contaminated by brine as it picks up sulfate and sodium relative to the dilution of the water by in-situ pore water.

Changes in the anion composition of pore water clearly show an increase in the concentration of sulfate ion in excess of the amount added from the brine. The mineralogy of the sediments has been studied, and sulfate minerals have not been identified by x-ray diffraction (Bartholomay 1990). Another source of sulfate is needed that might not be identified through x-ray diffraction. Atmospheric deposition is a possible source. Atmospheric deposition is recorded at Craters of the Moon National Monument, 24 mi southwest of the SDA (National Atmospheric Deposition Program 2003). The 20-year precipitation-weighted average composition of atmospheric deposition is shown in Table 5. If this water is evaporated to dryness, such as would happen in the upper layers of sediment during the summer, calcite and gypsum will form. If this is the sulfate source, this gypsum is either too amorphous or too rare to be detected by x-ray diffraction. Subsequent recharge dissolves some of the gypsum. Pore water at the SDA is mostly undersaturated with respect to gypsum (Table B-4, Appendix B), so this dissolution is thermodynamically possible. Additional work on the overall water and chemical mass balance is needed to further define this process.

4.2.1.3 Spatial Distribution. Because brine was used as a dust suppressant on roads, there should be a correlation between proximity to roads and brine contamination in lysimeters. Figure 15 shows a map of the SDA wells in the surficial sediment, and identifies those in which brine contamination was observed. Wells along the main east-west haul road, more or less congruent with 669500 N in Figure 15, show contamination with brine. The lysimeters along the roads are also in close proximity to drainage ditches that parallel the roads and carry rainfall and snowmelt runoff. This provides the double opportunity for contamination with brine; proximity to the source and enhanced infiltration from concentrated runoff in drainage. The distance from the wells to the nearest road is summarized in Table 6. The left two columns list wells that show contamination, and the right two columns show wells that are clean. On the average, contaminated wells are closer to roads than uncontaminated wells. What is the more important statistic, however, is the maximum distance from the road to the contaminated wells. There are three contaminated wells about 36–39 ft from roads. Clean wells that are closer to roads than 40 ft are all adjacent to roads where brine was not applied. Well W25 is 42 ft from a road treated with brine and is clean. From Table 6, we conclude that brine can move laterally distances on the order of 40 ft from roadways.

Cation	meq/L	Anions	meq/L
Calcium	0.122	Sulfate	0.114
Ammonia	0.108	Nitrate	0.109
Sodium	0.094	Chloride	0.093
Magnesium	0.026		
Potassium	0.008		



Contaminated with Brine		Uncontaminated with Brine	
Well	Distance to Nearest Road (ft)	Well	Distance to Nearest Road (ft)
98-1	86	C01	99
98-4	28	TH05	15
98-5	25	w02	273
PA01	39	W04	22
PA02	15	W06	16
TH04	36	W08	107
W03	4	W09	14
W05	10	W13	195
W23	12	W25	42
Average	28		87

An area with significant brine contamination is in the southeast corner of the SDA in wells W05, LYS-1, and 98-1. Brine was not applied inside the SDA in this area, but was applied to the road along the east boundary of the SDA in 1984 and 1985 (Figure 4). The distance to the road along the eastern boundary is 86 ft for well 98-1 and 170 ft for well W05. These are significantly greater distances than other brine-contaminated wells. During construction of the peripheral drainage channel, the locations of roads may have changed. Thus, brine may have been applied closer to these wells than the current distances indicate. High chloride concentrations in wells W05 and 98-1, however, indicate that the lateral spread of brine in sediments is still not well-constrained.

4.2.1.4 Temporal Changes. Brine was applied to roads between 1984 and 1993. Chloride is a conservative chemical species, and should be flushed out of the shallow vadose zone proportional to the water moving through the surficial sediment. Changes in concentrations of chloride with time in lysimeters can indicate the rate of flushing of the shallow vadose zone. Rates of infiltration through the surficial sediment at the SDA are highly variable (Martian 1995; Bishop 1998), and so different locations can be expected to see different amounts of brine leaching.

The first time series plot shown is for wells in the southeast corner of the SDA (Figure 16). Well W05 was drilled in 1986. There are three lysimeters installed in this well: (a) lysimeter L24 at a depth of 15.9 ft, (b) lysimeter L25 at a depth of 10.0 ft, and (c) lysimeter L26 at a depth of 6.7 ft. Well 98-1 was drilled in 1998 and has one lysimeter, L35, installed at 16.5 ft. Two lysimeters were installed in well LYS-1, located beside the beryllium blocks. These lysimeters are L40 at 6.6 ft and L41 at 19.7 ft. Quite a few samples were collected from well W05 in the 1980s, but only one sample has been collected from lysimeter W05-L25 since then. Three samples have been collected from lysimeter 98-1-L35. Two samples have been collected from lysimeter LYS-1-L41. Brine contamination was present in lysimeter W05-L25 at a depth of 10 ft in 1989, but was not present at a depth of 15.9 ft. Currently, based on one sample from 10 ft, brine appears to have migrated below a depth of 10 ft at lysimeter W05-L25. Samples from lysimeter 98-1-L35 indicate that brine is now at a depth of 16.5 ft. In LYS-1-L41, chloride concentration at 19.7 ft was 675 mg/L in 1997, and decreased to 102 mg/L in 2000. A lack of comparable data between wells, and the single recent sample from well W05, make it difficult to quantify the vertical movement of chloride at this site. Some lysimeters show decreasing chloride concentrations, while others show continued high concentrations.

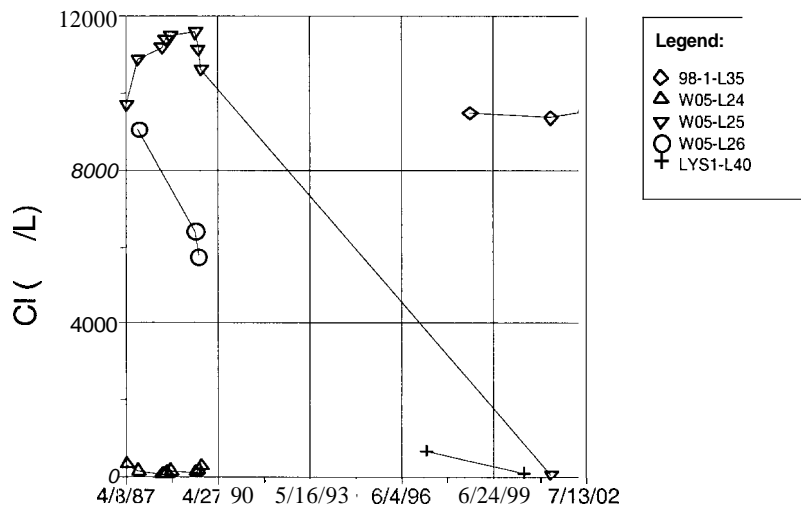


Figure 16. Time series plot of chloride concentrations in the south east corner of the SDA in wells 98-1, W05, and LYS-1.

The sulfate concentrations in wells W05 and 98-1 (Figure 17) show the same patterns as the chloride concentrations. Sulfate concentration has apparently decreased at a depth of 10 ft and is increasing at a depth of 16.5 ft. Comparable data from lysimeters L24 and L35 would provide significant information on whether the chloride front is migrating downward in the southeast corner of the **SDA**.

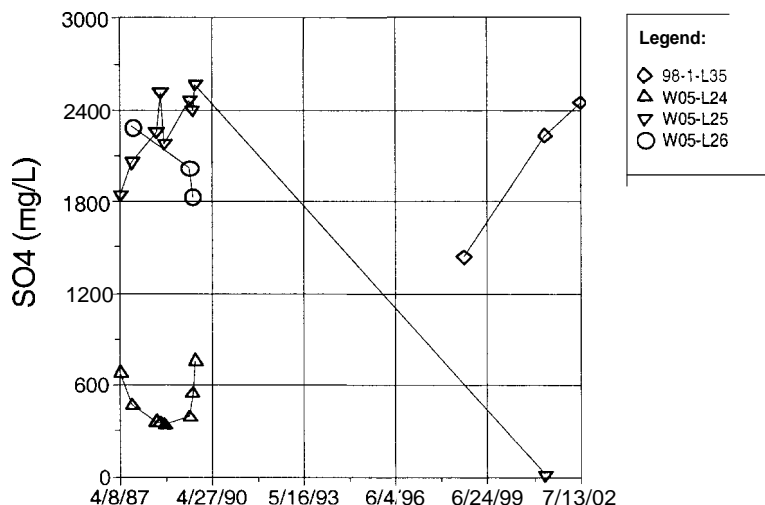


Figure 17. Time series plot of sulfate concentrations in the south-east corner of the SDA in wells 98-1 and W05.

Lysimeter L26 at a depth of 6.6 ft in well W05 contained over 8,000 mg/L chloride in 1987, less than three years after brine was applied to the road 86 ft east of this well. It does not seem likely that brine could move laterally that distance at that depth so rapidly. Two other wells containing lysimeters are located close to the southeast corner, but do not show elevated chloride concentrations. Lysimeters in wells W04 and W06 (Figure 18) are 40 mg/L chloride or less since installation in 1986. The low chloride concentrations in wells W04 and W06 indicate that the brine contamination in W05 is of very local extent, and may be related to movement of the road rather than migration of brine in the subsurface.

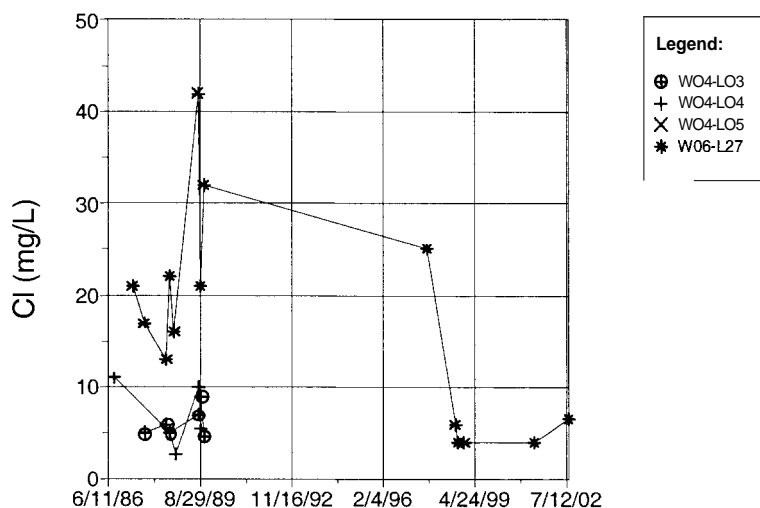


Figure 18. Time series plot of chloride concentrations in lysimeters at the southeast corner of the **SDA** that do not show brine contamination.

Another well with a good time history of chloride and sulfate concentrations is well W23 at the west end of the **SDA** (Figure 15). Well 23 was drilled in 1985 and has lysimeters installed at three depths: L07 at 18.8 ft, L08 at 11.8 ft, and L09 at 7.7 ft. Well 98-5 was drilled in 1998 and has one lysimeter, L39, installed at a depth of 10.5 ft. Both chloride (Figure 19) and sulfate (Figure 20) were elevated at depths of 7.7 ft and 11.8 ft in the late 1980s. A number of samples collected over the intervening years show a declining trend in both chloride and sulfate at both depths. Well 98-5 shows concentrations consistent with results from well W23. One sample has been collected from lysimeter L07 at a depth of 18.8 ft. This sample, collected in 2002, was also low in chloride and sulfate. These trends indicate that brine has been flushed from the shallow vadose zone in the west end of the **SDA**.

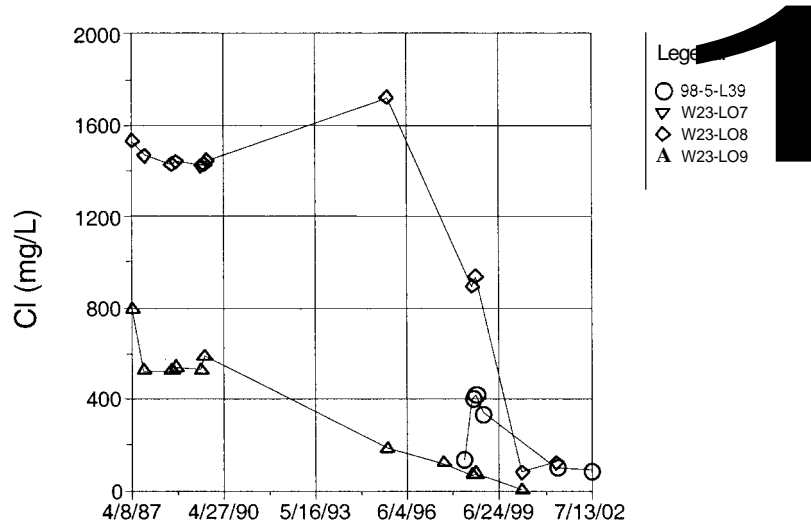


Figure 19. Time series plot of chloride concentrations at the west end of the **SDA** in wells W23 and 98-5.

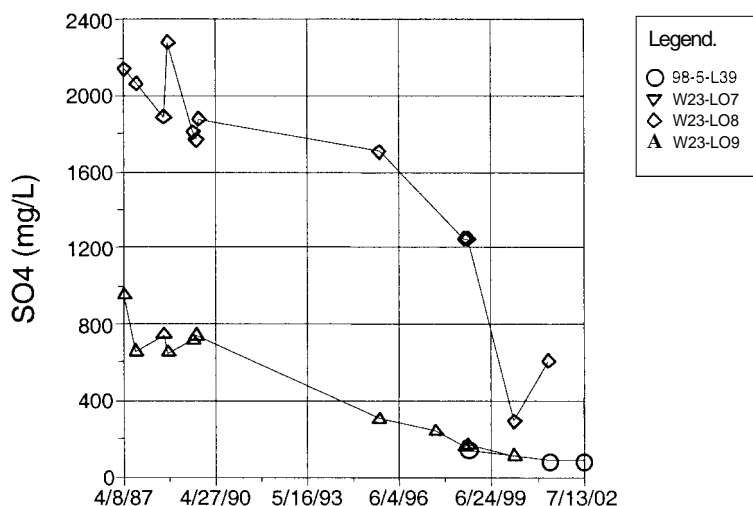


Figure 20. Time series plot of sulfate concentrations in the west end of the **SDA** in wells W23 and 98-5.

There are two lysimeters installed along the haul road near the center of the **SDA** along the southern edge of Pad A. These are lysimeter L15 in well PA01 and lysimeter L16 in well PA02 (Figure 15). A third lysimeter, L33, is installed at the northern edge of Pad A in well PA03. Lysimeter L33 was installed at a depth of 10 ft in 1994. Lysimeters L15 and L16 have the longest, and most

consistent, sampling record of any lysimeters at the **SDA**. Lysimeter L15 is at a depth of 14.3ft, and lysimeter L16 is at a depth of 8.7 ft. Both lysimeters showed elevated chloride concentrations in the 1980s (Figure 21), but not quite high enough to clearly conclude that this was from brine. Sulfate concentrations were also quite high in both lysimeters in the 1980s (Figure 22). In lysimeter L15, both chloride and sulfate decreased between sampling events in 1989 and 1994, indicating that the elevated concentrations probably were brine, and that the brine was being washed out of the sediment. Sulfate concentrations in lysimeter L16 also decrease significantly over this time period. Lysimeter L16 shows a significant increase in chloride concentration between 1989 and 1994, and continues to show high chloride concentrations (Figure 21). The increase in chloride, with the decrease in sulfate, indicates that this increase is probably not from brine contamination.

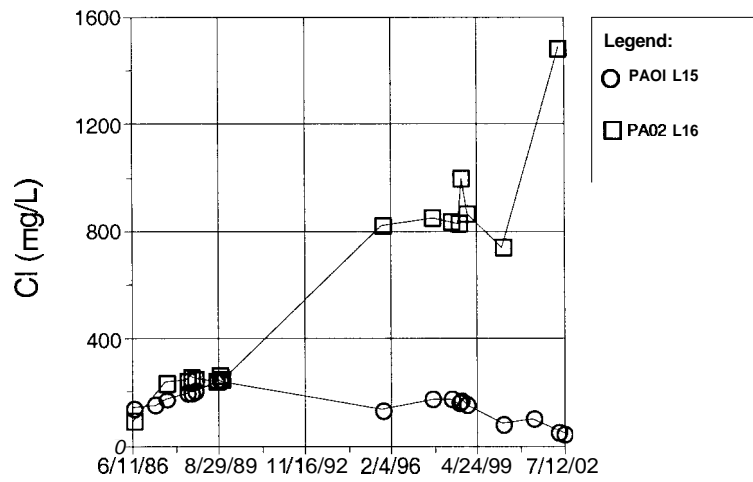


Figure 21. Time series plot of chloride concentrations near Pad A.

The waste in Pad A consists of sodium and potassium salts of nitrate, but is also high in sulfate and chloride (Shaw 1992). Sulfate and sodium do not show parallel increases to chloride in lysimeter L16, and so it is not clear that chloride is being released by waste in Pad A. By far the largest inventory on Pad A from an anion perspective is nitrate. Nitrate is also a conservative aqueous species under oxidizing conditions, and elevated nitrate levels would be expected along with chloride if the source of the elevated chloride was from Pad A.

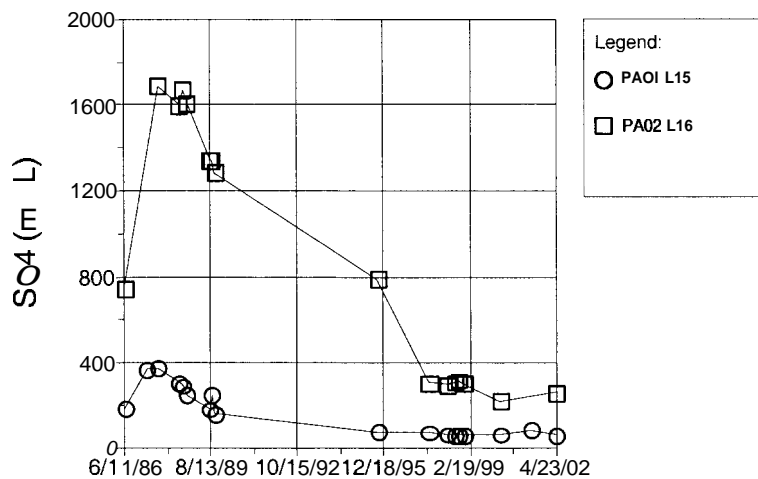


Figure 22. Time series plot of sulfate concentrations near Pad A.

Nitrate concentrations have been monitored around Pad A because nitrate salts are a significant portion of the waste stream disposed in Pad A. Nitrate and nitrite have been reported in a number of different concentration units over the years, and the exact correlation of units with measurements is not clear. There is a difference of **4.43** between nitrate concentrations reported as mg/L of nitrate and mg/L as nitrate-N. Results from the lysimeters around Pad A show significant fluctuations in nitrate-N concentration between sampling events (Figure 23). These fluctuations represent a change of about a factor of **4.4**. Therefore, it is likely that the fluctuations in reported nitrate-N concentration are an artifact of reporting unit uncertainty and not of actual changes in water chemistry. The higher concentrations probably represent nitrate as NO_3 rather than nitrate as N. The higher values are removed and the data replotted showing only the values that represent nitrate-N (Figure 24). With this selected subset of data, it appears that nitrate-N concentrations near Pad A have been stable for many years.

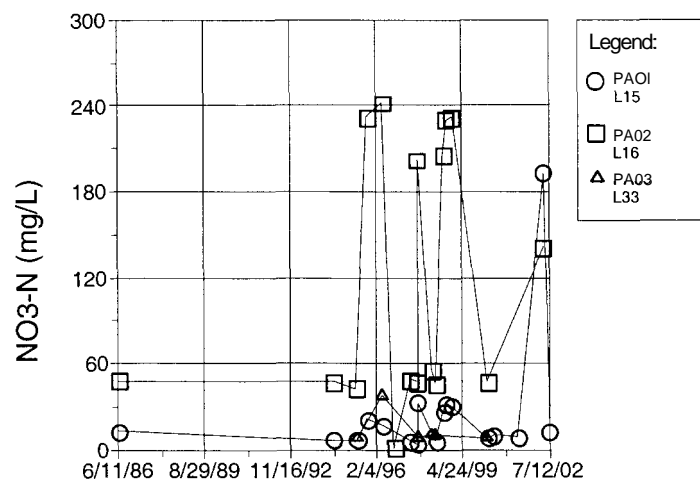


Figure 23. Time series plot of nitrate-N concentrations near Pad A for all reported nitrate data. Most of the fluctuations between sampling episodes vary by a factor of about 4.4 suggesting that the variation is from reporting units rather than changes in water chemistry.

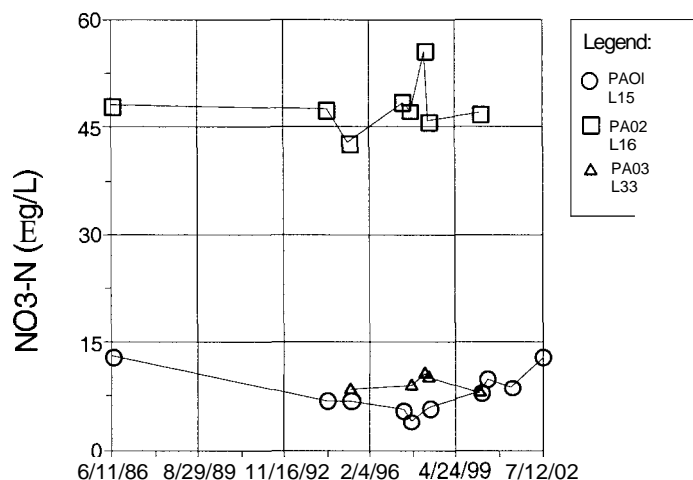


Figure 24. Time series plot of selected nitrate-N concentrations near Pad A.

Time series plots of chloride and sulfate concentrations in lysimeters indicate that the brine is being leached out of the surficial sediments at the **SDA**. Well W23, at the west end of the **SDA**, has returned to

levels that reflect natural pore water chemistry. At the southeast corner of the SDA, samples from wells W05 and LYS-1 indicate that brine has been leached from the system, but that an adjacent well still contains extremely high levels of chloride and sulfate. Lysimeter L16, adjacent to Pad A, shows increasing concentrations of chloride. This is not paralleled by increasing concentrations of sulfate or nitrate-N, so a brine source, or a source from Pad A, are not indicated.

4.2.2 Intermediate Vadose Zone

The intermediate vadose zone extends from the bottom of the surficial sediment to the B-C Sedimentary interbed (Figure 2). This includes the depth range from about 35 ft below land surface to a depth of about 140 ft below land surface. In addition to the B-C sedimentary interbed, there is a more shallow interbed at a depth of about 40 ft called the A-B interbed.

A few lysimeters were installed in this depth zone during the 1980s. Most of the lysimeters were installed in 1999 so there are only a few sampling points with any historical record. Where there were over 160 samples from the surficial sediment, there are only 15 samples collected before 1990 from a total of seven lysimeters installed in this depth interval (Table 7). In 1999 there were 11 additional lysimeters installed in this depth interval providing much broader coverage of the intermediate vadose zone. The seven lysimeters installed in 1986 and 1987 were installed in two wells, DO6 and TW1, in the north central portion of the SDA near Pad A (Figure 5), and in well D15 outside the south-west corner of the SDA.

Representative water analyses from the intermediate vadose zone are plotted on a Piper diagram in Figure 25. These chemical analyses are also presented in tabular form in Appendix B. There is a cluster of samples with over 50% of the anion equivalents from chloride in the lower right corner of the anion diagram. The waters not affected by brine show about an even mixture of anions, not the high bicarbonate shown in the near-surface water samples. The cations show a trend similar to the shallow vadose zone with a calcium-to-magnesium ratio of about 3 to 2, and a bias towards high sodium.

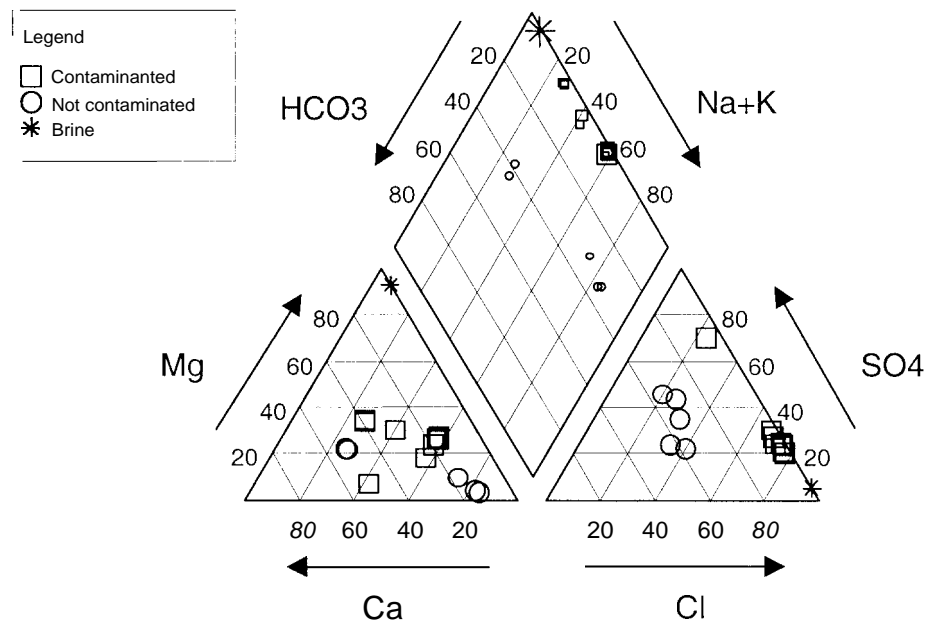


Figure 25. Piper diagram of waters in the intermediate vadose zone. The star represents the magnesium chloride brine, the squares are samples contaminated by the brine, and the circles are the unaffected waters. Symbol size in the triangle is proportional to chloride concentration, except for the brine.

Table 7. Summary statistics for water samples collected from suction lysimeters in the intermediate vadose zone at the SDA.

35 - 140'	Number of Samples			Detection Rates			Summary statistics			
	Before 1990	Since 1990	Total	Detected	Not Detected	% detects	Average of detects	Minimum of detects	Maximum of detects	Units
Bicarbonate	14	3	17	17	—	100%	230	121	449	mg/L
Bromide	11	26	37	29	8	78%	6.99	0.128	33	mg/L
Calcium	15	17	32	32	—	100%	277	35.2	911	mg/L
Chloride	14	26	40	40	—	100%	2180	0.987	7210	mg/L
Fluoride	14	22	36	27	9	75%	0.75	0.066	4.95	mg/L
Magnesium	15	17	32	32	—	100%	206	5.53	822	mg/L
Nitrate-N	—	36	36	32	4	89%	37.9	0.1	209	mg/L
Nitrite-N	—	30	30	9	21	30%	0.238	0.015	1.08	mg/L
pH (field)	10	1	11	11	—	100%	7.53	7.03	8.04	—
pH (lab)	13	2	15	15	—	100%	7.9	7.34	8.32	—
Phosphate	15	29	44	13	31	30%	0.338	0.012	1.88	mg/L
Potassium	15	17	32	32	—	100%	19.7	2.8	86.5	mg/L
SiO ₂	15	—	15	15	—	100%	79	73.3	83.5	mg/L
Sodium	15	17	32	32	—	100%	733	7.35	3180	mg/L
Sulfate	14	26	40	40	—	100%	1120	8.62	4400	mg/L
Temperature	10	1	11	11	—	100%	15.4	12	20.3	°C

The distribution of wells with elevated levels of chloride, indicating brine contamination, is shown in Figure 26. Wells around Pad A - D06, TW 1, and I-4S show elevated chloride levels, as do wells I-1S and O-4S at the west end of the SDA. Both of these well clusters in the intermediate vadose zone underlie areas in the shallow vadose zone that also show evidence of brine contamination.

Wells O-4S, I-1S, and I-4S were installed in 1999. Each well has only one chloride analysis. The lysimeters in wells D06 and TW 1 were installed in the late 1980s. There is a much longer record of water analyses from these wells. Water samples have been collected periodically from lysimeter DL02 (depth 44 ft) and DL04 (depth 102 ft). Both lysimeters showed elevated chloride and sulfate concentrations very soon after sampling started (Figures 27 and 28). The initial low concentrations probably reflect the distilled water used to wet the silica flour used in installing the lysimeter, rather than the initial breakthrough of the brine at this depth. There are a couple of 1988 samples from lysimeter DL01 (depth 88 ft) that show similar levels of chloride and sulfate at this intermediate depth near Pad A. Brine was first applied to roads in the SDA in 1984. By 1987, the brine was in lysimeters near Pad A at depths of 43 and 102 ft. Chloride and sulfate have persisted in these lysimeters since that time. In lysimeter DL02, at a depth of 43 ft, it appears that the chloride has started moving out of this depth interval. Chloride concentrations at a depth of about 100 ft at the west end of the SDA also indicate water movement through the vadose zone to this depth. From the single measurement to date, it is not possible to determine if the concentrations are changing.

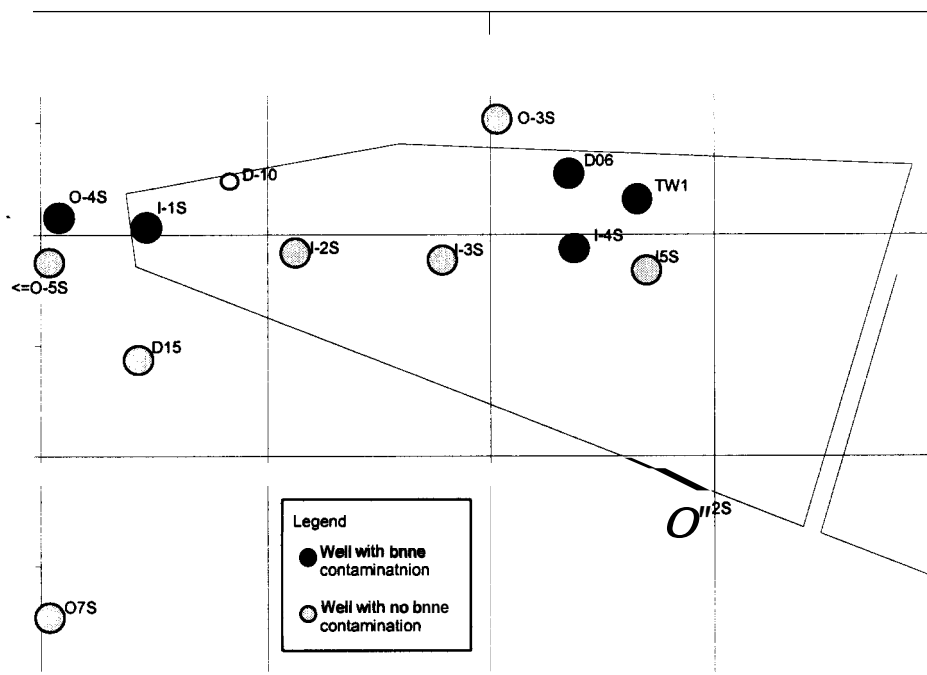


Figure 26. Map of the **SDA** showing the distribution of wells in the intermediate vadose zone contaminated by magnesium chloride brine.

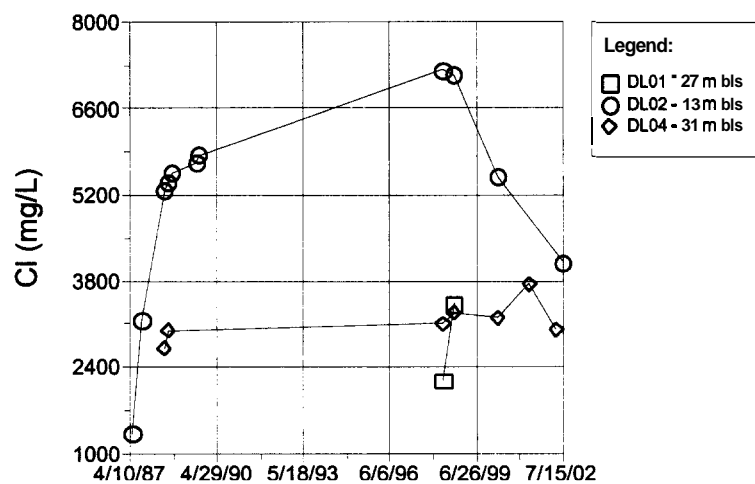


Figure 27. Time series plot of chloride concentrations in the intermediate vadose zone near Pad A.

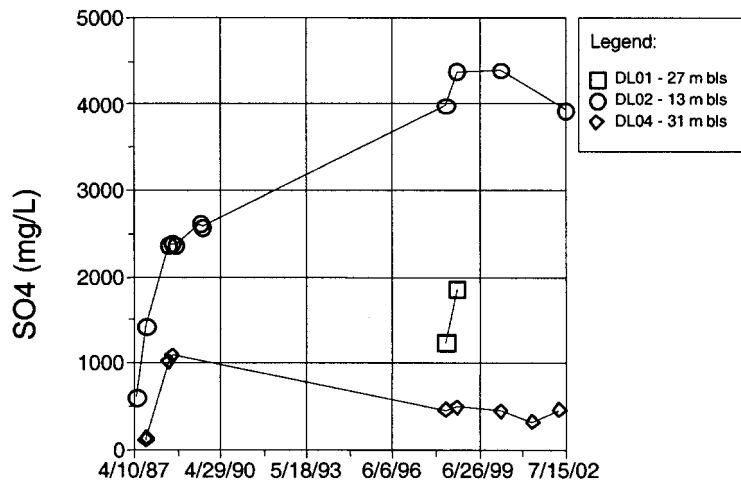


Figure 28. Time series plot of sulfate concentrations in the intermediate vadose zone near Pad A.

4.2.3 Deep Vadose Zone

The deep vadose zone extends from the bottom of the B-C sedimentary interbed to the water table (Figure 2). This includes the depth range from about 140 ft below land surface to the water table at a depth of about 600 ft below land surface. For this study, the most important sedimentary feature of this zone is the C-D sedimentary interbed at a depth of about 240 ft. Because of concerns with creating pathways through the C-D interbed for contaminant migration, very few wells have been drilled to depths greater than 250 ft inside the SDA.

Before 1999, there were only a few perched water wells completed in the deep vadose zone, and the water chemistry of this zone is not well-documented (Table 8). In 1999, an additional 11 lysimeters were installed in this zone (Figure 5).

Table 8. Summary statistics for water samples collected from suction lysimeters in the deep vadose zone at the SDA.

Analyte	Number of Samples			Detection Rates			Summary statistics			
	Before 1990	Since 1990	Total	Detected	Not Detected	% Detects	Average of detects	Minimum of detects	Maximum of detects	Units
Bicarbonate	—	2	2	2	—	100%	237	68	405	mg/L
Bromide	—	13	13	9	4	69%	1.17	0.102	5.49	mg/L
Calcium	1	18	19	19	—	100%	47.2	28.1	52.8	mg/L
Chloride	—	25	25	25	—	100%	271	20.5	3050	mg/L
Diss. Oxygen	1	—	1	1	—	100%	7.8	7.8	7.8	mg/L
Fluoride	—	13	13	10	3	77%	0.557	0.227	1.17	mg/L
Magnesium	1	18	19	19	—	100%	13.8	7.62	15.7	mg/L
Nitrate-N	—	20	20	18	2	90%	18.5	0.336	242	mg/L
Nitrite-N	—	14	14	2	12	14%	0.196	0.012	0.379	mg/L
pH (field)	1	2	3	3	—	100%	7.2	7.03	7.4	—
pH (lab)	1	—	1	1	—	100%	7.94	7.94	7.94	—
Phosphate	1	14	15	1	14	7%	0.02	0.02	0.02	mg/L

Table 8. (continued).

140 to 250 ft Analyte	Number of Samples		Detection Rates			Summary statistics				
	Before 1990	Since 1990	Total	Detected	Not Detected	% Detects	Average of detects	Minimum of detects	Maximum of detects	Units
Potassium	1	18	19	19	—	100%	3.09	2.57	6.29	mg/L
SiO ₂	1	—	1	1	—	100%	72.4	72.4	72.4	mg/L
Sodium	1	18	19	19	—	100%	24.5	6.48	222	mg/L
Sulfate	—	13	13	13	—	100%	664	32.3	5770	mg/L
Temperature	2	15	17	17	—	100%	10.4	8.1	12.5	°C

There is only one sample from this zone from before **1990**. The sample was collected from lysimeter DL03 in well TW1, near Pad **A** in **1988**. No anions were analyzed in the sample, so whether brine had reached this lysimeter cannot be determined. This lysimeter has not been sampled since, for cations or anions. There are no water analyses with a complete set of analyses for cations and anions, so a Piper diagram cannot be constructed for water in the deep vadose zone. There are 25 chloride analyses, with the maximum chloride concentration of over 3,000 mg/L, so there is evidence of brine migration to this depth. The distribution of wells with chloride over 350 mg/L is shown in Figure 29.

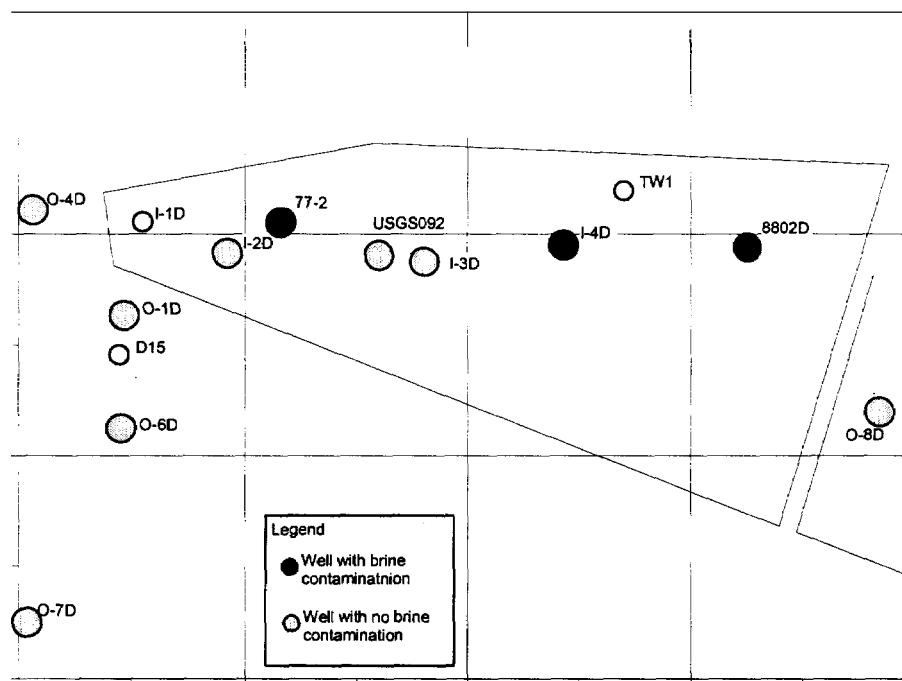


Figure 29. Map of the **SDA** showing the distribution of wells in the deep vadose zone contaminated by magnesium chloride brine.

The wells with brine contamination fall along the main haul road through the center of the **SDA**. Well **I-2D** contains 336 mg/L chloride, and may have a small amount of brine contamination. Almost all of the lysimeters in this depth interval were installed in **1999**. There is insufficient record to create time series plots for this depth interval.

5. MIGRATION RATES

From the measured chloride concentrations, bounding estimates of the downward percolation rate of water can be made. None of the chloride measurements can be identified as first arrival of chloride at a particular depth. Therefore, the calculated rates represent the lower bound of the chloride percolation rate. Arrival of chloride at a depth and time sooner than the measurement was made would require a faster percolation rate. All rates are calculated based on the assumption that the chloride detected in the lysimeters was from the August 1984 application. The distance to the sampling point must include both the vertical and lateral distance from the chloride source, which is assumed to be the haul road. The path water travels through the subsurface is unknown, so two distances are calculated. The shorter, or direct, distance assumes the water moves from the haul road directly to the sampling point. The longer distance assumes water travels vertically to depth, then horizontally to the well. Whether this occurs in a single step or a number of smaller steps does not affect the distance. The difference based on the two distances is fairly small.

The perched water monitoring wells 77-2 and 8802D are located very close to the haul road. As such, the migration is mainly downwards. The two lysimeters (DL02 and DL04) are located a ways north of the haul road, and so there is an appreciable lateral component of subsurface flow to reach these lysimeters. The fastest calculated rate is to the shallowest lysimeter (DL02) in the A-B interbed (Table 9). Rates for the deeper sampling points are lower. This likely reflects the rapid downward movement through the A basalt, with some slowing of water movement through the A-B and B-C interbeds. The rate of movement to lysimeter DL04 and to well 8802D decrease with depth, indicating impedance to vertical flow from interbeds. The higher calculated flow rates to the lysimeters may also reflect higher lateral flow rates, due to the anisotropy of the hydraulic conductivity of the basalts. The slower calculated rate of chloride movement to well 77-2, which is about the same depth as lysimeter DL04, could have more to do with local hydrogeologic conditions around the well than the depth.

Table 9. Estimates of water percolation rates for perched water wells and lysimeters completed in the intermediate and deep vadose zone.

Location	Date Cl measured (time, years)	Depth bls (ft)	Offset from haul road (ft)	Long distance to lysimeter or well (ft)	Overall rate (fb/yr)	Direct distance to lysimeter or well (ft)	Overall rate (ft/yr)
DL02 in well D06	May 1987 (2.8)	43	360	400	140	364	130
77-2	Apr 1990 (5.7)	89	72	160	28	115	20
DL04 in well TWO 1	June 1988 (3.8)	102	262	364	95	282	74
8802D	Jan 1990 (5.4)	220	33	253	46	223	41

In a computer simulation of water flow through the vadose zone at the SDA, Manguson and Sondrup (1998) calculated the residence time in the vadose zone under the SDA. They obtained different residence times for different grid blocks in the model depending on the subsurface geology and amount of surface recharge. The shortest residence times were for the grid block that encompasses well 8802D and lysimeters DL02 and DL04. The average percolation rate calculated from the modeled residence time is 25 fb/yr, in general agreement with the percolation rates for chloride to well 8802D and 77-2, where movement is primarily downwards.

6. GASES

In the vadose zone, the pores of the basalt and sediments are only partially filled with water, and there is a gas phase present. The composition of this gas phase plays an important role in the geochemical environment and affects the rate at which contaminants migrate. The microbial degradation of organic matter buried in the pits and trenches consumes oxygen and produces carbon dioxide. Corrosion of metals is enhanced if oxygen is present, so the distribution of gases in the vadose zone at the SDA is relevant to the question of corrosion. Data have been obtained for two of the important geochemical gases, oxygen and carbon dioxide, in the vadose zone.

6.1 Oxygen

Oxygen is an important factor in the oxidation potential of the vadose zone. Oxygen diffuses from the atmosphere through the open pores. Microbes in the vadose zone use the oxygen for metabolism. In the pits and trenches, there are large quantities of organic carbon in the form of cardboard boxes, plywood boxes, anticontamination clothing, rags, and trash. This provides a large sink for oxygen. Oxygen has been measured in lysimeter water samples by Winkler titration. Results of these analyses are plotted in Figure 30. At 5,000 ft above sea level, water in equilibrium with oxygen in the atmosphere will contain about **8.5 mg/L**. The measured oxygen concentration in the background lysimeter is near this value. Inside the SDA, the dissolved oxygen concentrations are lower than would be expected from equilibration with air. This indicates some consumption of oxygen. This is most likely the result of microbial degradation of organic matter in the pits and trenches in the SDA.

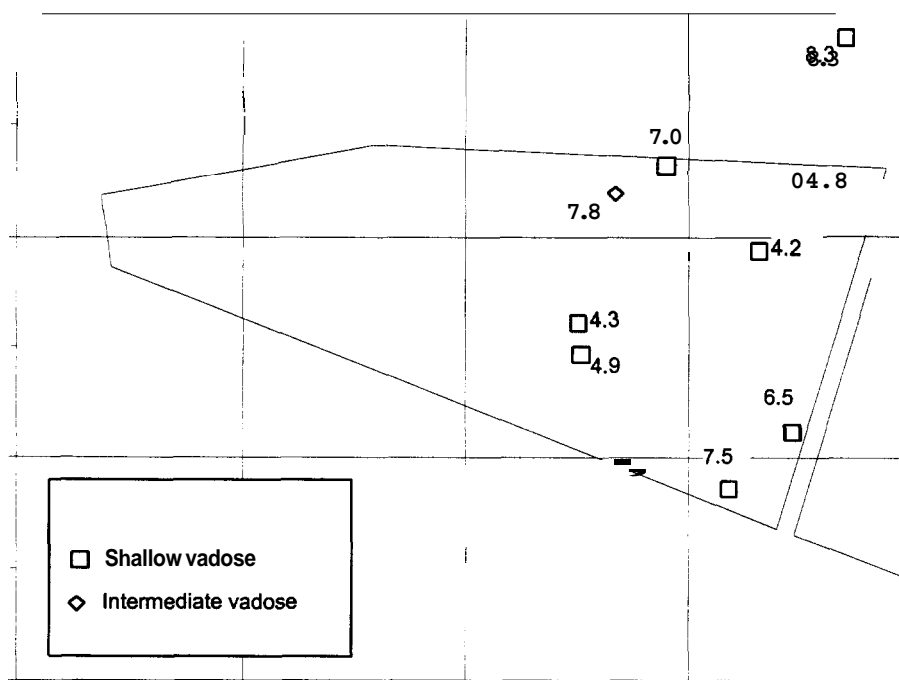


Figure 30. Map of the SDA showing the locations of the wells where dissolved oxygen has been measured and the concentrations of dissolved oxygen in mg/L. Water in equilibrium with air at an elevation of 5,000 ft would contain about **8.5 mg/L**.

6.2 Carbon Dioxide

An effective carbon dioxide partial pressure can be calculated from a water analysis using the pH and measured alkalinity. Where pH and alkalinity measurements were available, an effective partial pressure of carbon dioxide was calculated for lysimeter water. Figure 31 shows these calculated values. Carbon dioxide is given in parts per million by volume (ppmv) for a gas phase in equilibrium with the lysimeter water. Atmospheric concentration of carbon dioxide is about 360 ppmv. In the subsurface, microbial activity and plant root respiration increase carbon dioxide concentrations. In the background lysimeters, carbon dioxide concentrations range from 900 to 3,400 ppmv, slightly above atmospheric concentrations.

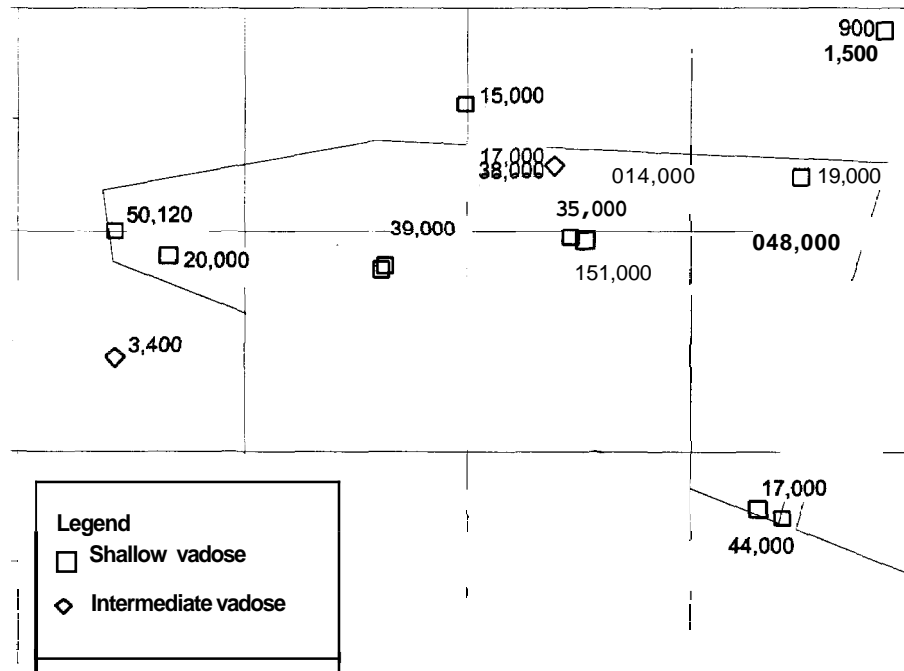


Figure 31. Map of the SDA showing the calculated partial pressure of carbon dioxide in ppmv in lysimeter water. The partial pressure of carbon dioxide in air is about 360 ppmv.

Inside the boundaries of the SDA, carbon dioxide concentrations in the gas phase are 10 to 40 times the background values, and 100 to 400 times atmospheric concentrations. These high concentrations are likely the result of carbon dioxide, generated in the pits and trenches from degradation of organic matter, diffusing out into the surrounding surficial sediments. Gas-phase concentrations of carbon dioxide would be much higher inside the pits and trenches.